nature immunology

The adaptor protein CARD9 is essential for the activation of myeloid cells through ITAM-associated and Toll-like receptors

Hiromitsu Hara[1,2], Chitose Ishihara[1], Arata Takeuchi[1], Takayuki Imanishi[1], Liquan Xue[3], Stephan W Morris[3], Masanori Inui[4], Toshiyuki Takai[4], Akira Shibuya[5], Shinobu Saijo[6], Yoichiro Iwakura[6], Naohito Ohno[7], Haruhiko Koseki[8], Hiroki Yoshida[2], Josef M Penninger[9] & Takashi Saito[1]

Immunoreceptor tyrosine-based activation motifs (ITAMs) are crucial in antigen receptor signaling in acquired immunity. Although receptors associated with the ITAM-bearing adaptors FcRγ and DAP12 on myeloid cells have been suggested to activate innate immune responses, the mechanism coupling those receptors to 'downstream' signaling events is unclear. The CARMA1–Bcl-10–MALT1 complex is critical for the activation of transcription factor NF-κB in lymphocytes but has an unclear function in myeloid cells. Here we report that deletion of the gene encoding the Bcl-10 adaptor–binding partner CARD9 resulted in impaired myeloid cell activation of NF-κB signaling by several ITAM-associated receptors. Moreover, CARD9 was required for Toll-like receptor–induced activation of dendritic cells through the activation of mitogen-activated protein kinases. Although *Bcl10*$^{-/-}$ and *Card9*$^{-/-}$ mice had similar signaling impairment in myeloid cells, *Card11*$^{-/-}$ (CARMA1-deficient) myeloid cell responses were normal, and although *Card11*$^{-/-}$ lymphocytes were defective in antigen receptor–mediated activation, *Card9*$^{-/-}$ lymphocytes were not. Thus, the activation of lymphoid and myeloid cells through ITAM-associated receptors or Toll-like receptors is regulated by CARMA1–Bcl-10 and CARD9–Bcl-10, respectively.

T cells and B cells, which are mainly responsible for regulating acquired immunity, are activated through T cell receptors (TCRs) and B cell receptors (BCRs). Those antigen receptors 'trigger' activation signals by associating with signaling molecules such as CD3 proteins or immunoglobulin-α (Igα) and Igβ, which contain immunoreceptor tyrosine-based activation motifs (ITAMs) in their cytoplasmic domains[1]. The activation signal is transduced by the phosphorylation of specific tyrosine residues in the ITAMs and subsequent recruitment of the tyrosine kinases Syk or Zap70 to the phosphorylated ITAMs. In addition to lymphocytes, natural killer cells and myeloid lineage cells such as mast cells, macrophages, neutrophils and dendritic cells (DCs)[2] also express receptors that transduce their signals through ITAMs and regulate cell functions in innate immunity.

Two ITAM-containing adaptor proteins, DAP12 and FcRγ, are known to associate with receptors in myeloid cells (ITAM-associated receptors); for the myeloid receptors, signaling from the receptor is mediated by the ITAM-containing adaptors and subsequently leads to Syk activation. FcRγ is required for the activation of Fc receptors on myeloid cells, including FcγRI (CD64) and FcγRIII (CD16) for IgG, and FcεRI for IgE. Other FcRγ-associated activation receptors expressed on myeloid cells include PIR-A[3,4], LIR[5], DCAR[6] and OSCAR[7]. DAP12-associated myeloid receptors include the TREM family of receptors[8], MDL-1 (ref. 9), SIRP-β[10], PILRβ[11], IREM2 (ref. 12), CD200R[13] and MAIR-II (LMIR-2)[14].

Stimulation of those FcRγ- or DAP12-associated receptors on myeloid cells induces various signaling pathways leading to the production of cytokines and/or chemokines. FcγRI- and FcγRIII-mediated activation of macrophages triggers the generation of inflammatory cytokines and reactive oxygen species[15]. OSCAR stimulation leads to cytokine release and DC survival through the activation of pathways dependent on the kinase Erk and phosphatidylinositol-3-OH kinase[16]. Ligation of TREM-1 induces the production of inflammatory chemokines and cytokines such as interleukin 8 (IL-8) and myeloperoxidase in neutrophils and monocytes as well as the

[1]Laboratory for Cell Signaling, RIKEN Research Center for Allergy and Immunology, Yokohama, Kanagawa 230-0045, Japan. [2]Department of Biomolecular Sciences, Faculty of Medicine, Saga University, Saga, Saga 849-8501, Japan. [3]Department of Pathology and Oncology, St. Jude Children's Research Hospital, Memphis, Tennessee 38105, USA. [4]Department of Experimental Immunology, Institute of Development, Aging and Cancer, Tohoku University, Sendai, Miyagi 980-8575, Japan. [5]Department of Immunology, Institute of Basic Medical Sciences, University of Tsukuba, Tsukuba, Ibaraki 305-8575, Japan. [6]Center for Experimental Medicine, The Institute of Medical Science, The University of Tokyo, Minato-ku, Tokyo 108-8639, Japan. [7]Laboratory for Immunopharmacology of Microbial Products, School of Pharmacy, Tokyo University of Pharmacy and Life Science, Hachioji, Tokyo 192-0392, Japan. [8]Laboratory for Developmental Genetics, RIKEN Research Center for Allergy and Immunology, Yokohama, Kanagawa 230-0045, Japan. [9]Institute of Molecular Biotechnology of the Austrian Academy of Sciences, 1030 Vienna, Austria. Correspondence should be addressed to T.S. (saito@rcai.riken.jp) or H.H. (harah@cc.saga-u.ac.jp).

Received 23 January; accepted 13 April; published online 7 May 2007; doi:10.1038/ni1466

production of chemotactic protein 1 and tumor necrosis factor (TNF) in monocytes[17]. Studies demonstrating that treatment of mice with a soluble TREM-1–Ig fusion protein can prevent death by lipopolysaccharide (LPS)–induced septic shock suggest involvement of TREM-1 in amplifying LPS signals[18]. Triggering MAIR-II also induces the secretion of proinflammatory cytokines and/or chemokines from macrophages[14]. Moreover, ITAM-associated receptor–mediated stimulation has been also shown to induce DC maturation[16,17]. Thus, signals through the ITAM-associated receptors mediate the activation and maturation of macrophages and DCs. However, the molecular mechanisms underlying the coupling of the ITAM-associated receptor triggering to the induction of inflammatory gene expression have remained poorly understood.

In addition to the ITAM-associated receptors discussed above, myeloid cells express DC-associated C-type lectin 1 (dectin-1), which contains an atypical ITAM in its cytoplasmic tail[19]. Unlike typical ITAMs, which require two phosphorylated tyrosine residues in the motif for Syk recruitment, only one tyrosine is required for the recruitment of Syk to the dectin-1 atypical ITAM. Dectin-1 is a pattern-recognition receptor for β-glucan mainly present in the fungal cell wall. Zymosan, a yeast cell wall extract composed mainly of β-glucan and other various components, can stimulate dectin-1 to produce inflammatory cytokines such as IL-2, TNF, IL-6, IL-10 and IL-12. It has been shown that zymosan can also stimulate Toll-like receptor 2 (TLR2) to produce certain cytokines such as TNF and IL-12 through the activation of NF-κB mediated by the adaptor protein MyD88 (myeloid differentiation primary-response gene 88)[20]. It has been suggested that dectin-1 induces both Syk-dependent and Syk-independent signaling pathways in macrophages and DCs. Although cooperative signaling is required with TLR2, dectin-1-induced production of IL-12 and TNF is Syk independent, whereas IL-2 and IL-10 production is Syk dependent[21]. However, how dectin-1-mediated signals integrate with TLR signals and the mechanism by which the Syk-dependent and Syk-independent pathways are regulated to trigger different sets of cytokine genes are unknown.

The caspase-recruitment domain (CARD) is a protein-binding module that mediates the assembly of CARD-containing proteins. One of the CARD proteins, Bcl-10 (ref. 22), functions together with the MALT1 adaptor protein[23,24] as a central regulator of TCR- and BCR-mediated NF-κB activation. In addition, it has been shown that NF-κB activation mediated by Bcl-10 and that MALT1 is also critical for FcεRI-induced cytokine production and late-phase anaphylactic reactions[25]. Thus, these studies indicate the possibility that the Bcl-10–MALT1 complex is critical for ITAM-mediated NF-κB activation in other type of cells as well as lymphocytes.

CARMA1 (also called CARD11 and Bimp3), a CARD-containing protein of the MAGUK (membrane-associated guanylate kinase) family, is essential for TCR- and BCR-induced NF-κB activation and acquired immunity through the regulation of protein kinase C (PKC)–dependent lipid raft recruitment of Bcl-10 and inhibitor of NF-κB (IκB) kinase (IKK) proteins[26,27]. The three adaptors, CARMA1, Bcl-10 and MALT1, thus interact with each other to form a complex, called the CARMA1–Bcl-10–MALT1 (CBM) complex. Involvement of the CBM complex in TLR4 signaling in B cells has been demonstrated[23,26,28].

CARD9 is structurally related to CARMA1 and is expressed in a variety of human tissues, including peripheral blood lymphocytes and spleen[29]. Like CARMA1, CARD9 associates with Bcl-10 through its CARD and synergistically induces NF-κB activation[29]. Analysis of *Card9*$^{-/-}$ mice has shown that CARD9 is involved in antifungal immunity[30]. CARD9 has been suggested to mediate signals from dectin-1 to NF-κB activation through its atypical ITAM and Syk, as *Card9*$^{-/-}$ macrophages show impaired NF-κB activation and cytokine production in response to zymosan and *Candida albicans*. However, it has been suggested that TNF production and NF-κB activation of macrophages after zymosan stimulation is dependent mainly on MyD88-mediated signaling[31]. Moreover, dectin-1 deficiency does not alter the production of TNF and IL-12 by macrophages and DCs after zymosan stimulation or the defense against *C. albicans*[32]. These reports suggest that the impairment of cytokine responses to zymosan and defense against *C. albicans* of *Card9*$^{-/-}$ mice is not simply due to impairment of the dectin-1–Syk–CARD9 signaling pathway. Therefore, the physiological functions of CARD9 in various innate immune responses remain to be determined. In addition, the functional relationship of CARD9 with CBM-mediated regulation needs to be defined to clarify CARD9-mediated signaling.

Here we report studies of *Card9*$^{-/-}$, *Card11*$^{-/-}$ (CARMA1-deficient) and *Bcl10*$^{-/-}$ mice showing that the signaling pathway through CARD9–Bcl-10 but not through CARMA1–Bcl-10 was essential for myeloid cell activation mediated by various FcRγ- and/or DAP12-associated receptors. Loss of either CARD9 or Bcl-10 abrogated ITAM-associated receptor–mediated inflammatory cytokine responses in macrophages and DCs because of impaired NF-κB activation. CARD9 deficiency impaired cytokine production through both dectin-1- and MyD88-mediated signaling pathways after zymosan stimulation in DCs. Moreover, the CARD9–Bcl-10 pathway was involved in various TLR responses in DCs but not in lymphocytes through the activation of mitogen-activated protein kinases (MAPKs). Although CARD9 was dispensable for TCR- and BCR-mediated acquired immunity, CARMA1 deficiency did not affect cytokine responses in myeloid cells mediated by ITAM receptors (that is, ITAM-associated and ITAM-bearing receptors) or TLRs. Thus, we provide here genetic evidence for differential requirements of CARD9 and CARMA1 in Bcl-10-mediated activation of myeloid cells and lymphoid cells, respectively.

RESULTS

Generation of CARD9-deficient mice

As with human CARD9 (ref. 29), bone marrow and spleen have very high expression of mouse CARD9, but it is barely detectable in thymus and lymph nodes, among the lymphoid organs (**Supplementary Fig. 1a** online). In the various hematopoietic cell populations, myeloid lineage cells such as macrophages, DCs and neutrophils have higher expression of CARD9 than do lymphocytes and mast cells (**Supplementary Fig. 1a**). To study the physiological function of CARD9, we generated CARD9-deficient (*Card9*$^{-/-}$) mice. As it has been shown that the CARD motif is an essential domain for Bcl-10–CARD9 interaction and NF-κB activation[29], we deleted exon 2 of mouse *Card9*, which encodes the CARD (**Supplementary Fig. 1b**). We confirmed gene targeting by Southern blot analysis (**Supplementary Fig. 1c**) and verified the null mutation of *Card9* by the absence of CARD9 by immunoblot analysis (**Supplementary Fig. 1d**). *Card9*$^{-/-}$ mice were born at the expected mendelian ratio and did not show any anatomic abnormalities.

CARD9 is dispensable for lymphocyte development and activation

Because CARD9 associates with Bcl-10 and Bcl-10 deficiency affects early thymic development, with more cells of the CD44$^-$CD25$^-$ subset in the CD4$^-$CD8$^-$ double-negative population[22], we first determined whether CARD9 deletion affected T cell development. *Card9*$^{-/-}$ mice had normal development of CD4$^-$CD8$^-$, CD4$^+$CD8$^+$, CD4$^+$CD8$^-$ and CD4$^-$CD8$^+$ cells in the thymus and of CD44$^+$CD25$^-$, CD44$^+$CD25$^+$,

$CD44^-CD25^+$ and $CD44^-CD25^-$ subsets in the double-negative populations (**Supplementary Fig. 2a** online). Moreover, the percentages (**Supplementary Fig. 2b**) and numbers (**Supplementary Fig. 2c**) of peripheral $CD3^+$ cells and of the $CD4^+$ and $CD8^+$ subsets of T cells were similar in *Card9*$^{-/-}$ and wild-type mice. As Bcl-10-mediated NF-κB activation is essential for T cell activation by TCRs, we next analyzed TCR-induced T cell activation in *Card9*$^{-/-}$ mice. *Card9*$^{-/-}$ T cells showed normal proliferation after stimulation with antibody to CD3 (anti-CD3) alone, with anti-CD3 plus anti-CD28 or with phorbol 12-myristate 13-acetate plus ionomycin (**Fig. 1a**). Consistent with those observations, the production of IFN-γ (**Fig. 1b**) and IL-2 (data not shown) and upregulation of the surface activation markers CD25, CD44 and CD69 (data not shown) after TCR stimulation were similar in wild-type and *Card9*$^{-/-}$ mice. Similarly, *Card9*$^{-/-}$ T cells had normal major histocompatibility complex–dependent responses to allogenic antigen-presenting cells (**Fig. 1c**) and the 'superantigen' staphylococcal enterotoxin B (**Fig. 1d**). These results demonstrate that CARD9 is dispensable for T cell development and TCR-mediated activation.

It has been reported that deficiency of Bcl-10, CARMA1 or MALT1 results in fewer mature $IgD^{hi}IgM^{lo}$ B cells and a lack of the $CD21^{hi}CD23^{lo}$ subset of marginal zone B cells in the spleen[23,26,28], suggesting that Bcl-10-mediated signaling is required for the peripheral differentiation of B cells. We therefore next examined whether CARD9 is involved in B cell development. B cell development in the bone marrow (**Supplementary Fig. 2d**) and numbers of $B220^+$ cells (**Supplementary Fig. 2e**) and $IgD^{hi}IgM^{lo}$ B cells and marginal zone B cells (**Supplementary Fig. 2f**) in the spleen were similar in *Card9*$^{-/-}$ and wild-type mice. As CARMA1–Bcl-10–mediated signaling is essential for BCR-, CD40- and TLR-induced B cell responses[22,23,26,28], we next analyzed the effect of CARD9 deficiency on B cell activation. The proliferation of splenic B cells after stimulation with anti-IgM (**Fig. 1e**), anti-CD40 (**Fig. 1f**), LPS or CpG DNA (**Fig. 1g**) was similar in *Card9*$^{-/-}$ and wild-type mice. Furthermore, *in vivo* antibody responses after immunization with the T cell–dependent antigen DNP-KLH (dinitrophenol–keyhole limpet hemocyanin) demonstrated normal production of DNP-specific IgM, IgG1, IgG2a and IgG3 in *Card9*$^{-/-}$ mice (**Fig. 1h**). These data

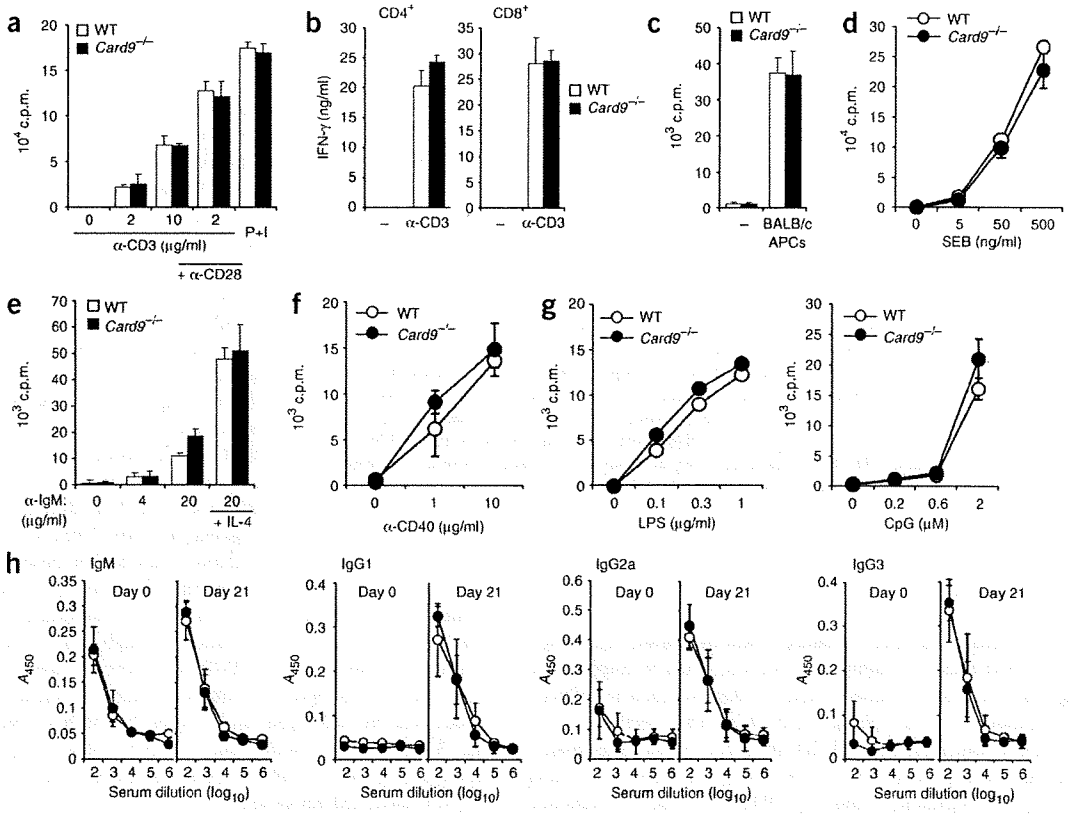

Figure 1 Normal activation of T and B lymphocytes in *Card9*$^{-/-}$ mice. (**a**) Proliferation of purified wild-type (WT) and *Card9*$^{-/-}$ T cells after stimulation with anti-CD3 alone (α-CD3; concentration, horizontal axis), anti-CD3 plus anti-CD28 (1 μg/ml; +α-CD28), or phorbol 12-myristate 13-acetate (10 ng/ml) plus ionomycin (1 μM; P+I). (**b**) ELISA of IFN-γ production by purified $CD4^+$ or $CD8^+$ lymph node T cells from wild-type and *Card9*$^{-/-}$ mice after 48 h of stimulation with anti-CD3 (α-CD3) or no stimulation (–). (**c**) Allogenic proliferative responses of wild-type and *Card9*$^{-/-}$ T cells after stimulation with irradiated spleen cells (APCs) from BALB/c mice or no stimulation (–). (**d**) Proliferation of T cells from wild-type or *Card9*$^{-/-}$ mice after stimulation with staphylococcal enterotoxin B (SEB) plus syngenic antigen-presenting cells. (**e–g**) Proliferation of purified wild-type and *Card9*$^{-/-}$ splenic B cells stimulated with the following: anti-IgM with (+ IL-4) or without recombinant IL-4 (10 ng/ml; **e**); anti-CD40 (**f**); LPS (**g**, left); or CpG DNA (**g**, right). (**h**) ELISA of serum titers of anti-DNP IgM, IgG1, IgG2a and IgG3 from wild-type mice (open circles; $n = 6$) or *Card9*$^{-/-}$ mice (filled circles; $n = 6$) immunized intraperitoneally with DNP-KLH on day 21 after immunization. A_{450}, absorbance at 450 nm. Data are the mean ± s.d. of triplicates (**a–g**) or six mice (**h**) and are representative of three (**a,b,e–g**), two (**c,d**) or one (**h**) independent experiment(s).

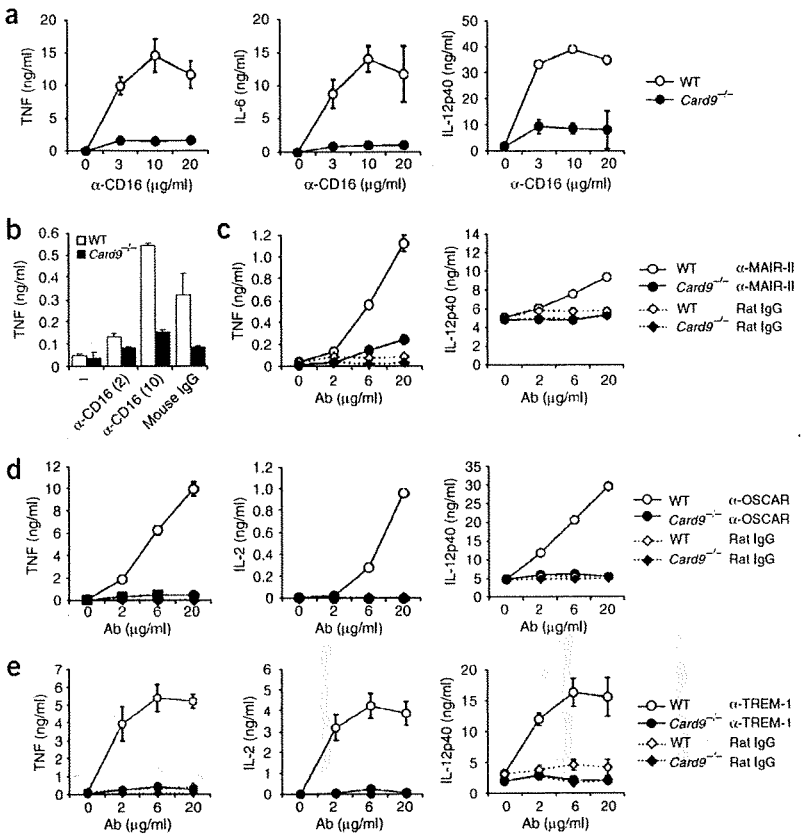

Figure 2 Impaired cytokine production by *Card9*$^{-/-}$ myeloid cells after stimulation through ITAM receptors. (**a**,**b**) ELISA of the production of TNF, IL-6 and/or IL-12p40 by wild-type or *Card9*$^{-/-}$ BMDCs (**a**) or bone marrow–derived macrophages (**b**) stimulated by crosslinking of FcγR with immobilized monoclonal anti-CD16 (α-CD16) or mouse IgG. – (**b**), no antibody; numbers in parentheses (**b**), concentration of anti-CD16 (in μg/ml). (**c**–**e**) ELISA of the production of TNF, IL-2 and IL-12p40 by wild-type and *Card9*$^{-/-}$ BMDCs after stimulation in the presence of FcR blocker (soluble mouse γ-globulin; 10 μg/ml) with immobilized monoclonal anti-MAIR-II (**c**), anti-OSCAR (**d**) or anti-TREM-1 (**e**). Rat IgG, control for stimulation. Ab (horizontal axes, **c**–**e**), antibody concentration. Data are the mean ± s.d. of triplicates and are representative of three independent experiments.

indicate that CARD9 is not involved in the development and activation of B cells.

Card9$^{-/-}$ myeloid cells have impaired ITAM-mediated signaling

Because myeloid cells had highly expression of CARD9 (**Supplementary Fig. 1a**), we next examined whether CARD9 deficiency affected the development of macrophages and DCs. The development of CD11b^{+}CD11c^{-} macrophages and CD11b^{-}CD11c^{+} DCs (**Supplementary Fig. 2g**), of subsets of CD4^{+}, CD8^{+} and CD4^{-}CD8^{-} cells among the CD11c^{+} DC populations and of CD11c^{+}CD19^{-}B220^{+} plasmacytoid DCs (**Supplementary Fig. 2h**) in the spleen was similar in *Card9*$^{-/-}$ and wild-type mice. Because it has been suggested that Bcl-10 is involved in FcR-mediated NF-κB activation in mast cells[25], we tested whether CARD9 is involved in FcR-mediated activation in myeloid cells. We prepared bone marrow–derived DCs (BMDCs) from *Card9*$^{-/-}$ mice and stimulated the cells by crosslinking of FcγRIII with monoclonal anti-CD16 or immobilized IgG. BMDCs developed normally from *Card9*$^{-/-}$ mice (**Supplementary Fig. 2i**). However, *Card9*$^{-/-}$ DCs had impaired production of TNF, IL-6 and IL-12 (**Fig. 2a**) after FcγR crosslinking. There was similar severe impairment in bone marrow–derived macrophages (**Fig. 2b**), suggesting that CARD9 is essential for FcγR signaling in myeloid cells. These results demonstrate that signals mediated through FcγR, which associates with ITAM-containing FcRγ, are impaired in *Card9*$^{-/-}$ DCs and macrophages, whereas TCR- and BCR-mediated signals in *Card9*$^{-/-}$ lymphocytes are unaffected. This suggests the possibility that CARD9 is involved in signaling through receptors associated with the ITAM-containing adaptors FcRγ or DAP12 specifically in myeloid cells.

CARD9 is involved in signaling from dectin-1, which contains an atypical ITAM in its cytoplasmic domain[30]. However, because of the unique features of dectin-1 in terms of the atypical ITAM, which requires phosphorylation of only a single tyrosine in the motif for Syk recruitment, that conclusion might be specifically restricted to dectin-1 and it may not be possible to generalize it to receptors associated with FcRγ and DAP12. To test that, we analyzed the surface expression of several receptors associated with FcRγ or DAP12 on BMDCs using specific monoclonal antibodies and verified expression of MAIR-II, OSCAR and TREM-1. Whereas MAIR-II and TREM-1 are associated with DAP12 (refs. 8,14), OSCAR is associated with FcRγ[7]. To determine whether CARD9 is involved in signaling through those ITAM-bearing receptors, we stimulated *Card9*$^{-/-}$ and wild-type BMDCs with monoclonal antibodies specific for MAIR-II (**Fig. 2c**), OSCAR (**Fig. 2d**) or TREM-1 (**Fig. 2e**). After crosslinking of MAIR-II, OSCAR and TREM-1, the production of all cytokines examined, including TNF, IL-2, IL-12 (**Fig. 2c**–**e**) and IL-6 (data not shown), was abrogated in *Card9*$^{-/-}$ BMDCs. Those defects were not overcome by stimulation with higher doses of antibodies, suggesting that CARD9 is crucial for cytokine production after stimulation of those FcRγ- and DAP12-associated receptors in BMDCs. In contrast to stimulation through ITAM-associated receptors, stimulation with anti-CD40 or phorbol 12-myristate 13-acetate plus calcium ionophore induced similar amounts of cytokine production in wild-type and *Card9*$^{-/-}$ BMDCs (**Supplementary Fig. 3** online), indicating that *Card9*$^{-/-}$ BMDCs are capable of producing cytokines and the defect is specific for ITAM-associated receptor–mediated activation.

Dectin-1- and MyD88-dependent DC activation requires CARD9

Consistent with a published report[30], zymosan-induced production of TNF, IL-2 (**Fig. 3a**) and IL-6 (data not shown) was considerably impaired in *Card9*$^{-/-}$ BMDCs. However, notably, IL-12 production after stimulation with zymosan seemed to be normal (**Fig. 3a**), in contrast to the response to stimulation through FcRγ- and DAP12-associated receptors, which resulted in impaired IL-12 production similar to that of other cytokines (**Fig. 2**). Zymosan, a polysaccharide

particle from the cell walls of *Saccharomyces cerevisiae*, is the most commonly used β-glucan-containing experimental reagent, but it contains other components, including other glucans, mannans, chitins and unknown TLR2 and TLR6 ligands[33,34]. It has been reported that zymosan-induced production of TNF and IL-12 requires the 'collaboration' of dectin-1 and TLR2, followed by activation of NF-κB through MyD88 (ref. 31). Indeed, it has been suggested that production of TNF and IL-12 after zymosan stimulation is impaired by MyD88 deficiency but not by dectin-1 or Syk deficiency[21,32]. Thus, it was not apparent if the impaired cytokine responses of *Card9*$^{-/-}$ BMDCs were due to a defect in the pathway of dectin-1–Syk signaling and/or TLR-MyD88 signaling.

To clarify that point, we compared cytokine responses of *Card9*$^{-/-}$, *Myd88*$^{-/-}$ and *Clec7a*$^{-/-}$ (dectin-1-deficient) BMDCs after stimulation with untreated zymosan or NaClO-oxidized zymosan. We generated NaClO-oxidized zymosan by treating zymosan with 0.5% NaClO and 0.1 M NaOH; it represents a product composed mainly of β-glucans[35] and therefore it specifically binds to dectin-1 but not TLRs. We found that zymosan-induced production of TNF, IL-6 and IL-12 was not impaired much in *Clec7a*$^{-/-}$ BMDCs (**Fig. 3b**). In contrast, production of TNF and IL-6 was much lower in *Myd88*$^{-/-}$ BMDCs, similar to that in *Card9*$^{-/-}$ BMDCs, whereas IL-12 was slightly lower in *Myd88*$^{-/-}$ BMDCs (**Fig. 3b**). These results indicate that zymosan stimulates production of TNF and IL-6 mainly through the TLR-MyD88 signaling pathway, not through the dectin-1-mediated pathway; they also suggest that CARD9 contributes TLR-MyD88 signaling rather than to dectin-1 signaling after zymosan stimulation. In contrast, all of cytokine responses to NaClO-oxidized zymosan were abolished in *Clec7a*$^{-/-}$ and *Card9*$^{-/-}$ BMDCs but not in *Myd88*$^{-/-}$ BMDCs (**Fig. 3c**), indicating that cytokine production after β-glucan stimulation is completely dependent on the dectin-1–CARD9 signaling pathway. Our data collectively indicate that CARD9 is indispensable for myeloid cell activation through ITAM-bearing dectin-1 and that CARD9 is also involved in TLR-MyD88 signaling.

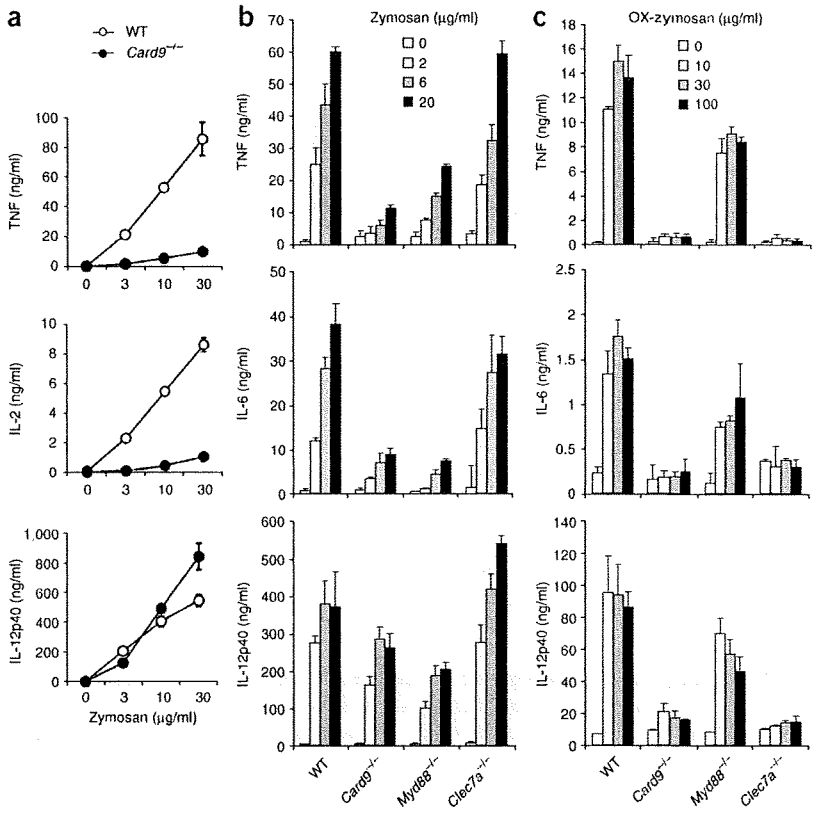

Figure 3 CARD9 is required for both MyD88- and dectin-1-mediated cytokine responses. (**a**) ELISA of the production of TNF, IL-2 and IL-12p40 by zymosan-stimulated wild-type or *Card9*$^{-/-}$ BMDCs. (**b,c**) ELISA of the production of TNF, IL-6 and IL-12p40 by wild-type, *Card9*$^{-/-}$, *Myd88*$^{-/-}$ or *Clec7a*$^{-/-}$ BMDCs in response to zymosan (**b**) or NaClO-oxidized zymosan (OX-zymosan; **c**). Data are the mean ± s.d. of triplicates and are representative of two independent experiments.

ITAM-mediated activation of NF-κB requires CARD9

We next analyzed the mechanism of impaired signaling in *Card9*$^{-/-}$ myeloid cells. As the CBM complex is essential for the coupling of antigen receptors to the activation of NF-κB and MAPK in T lymphocytes and B lymphocytes[24,26], we investigated the function of CARD9 in the ITAM-associated receptor–induced activation of NF-κB and MAPK in BMDCs through crosslinking of FcγR. Degradation of IκBα induced by FcγR crosslinking was impaired in *Card9*$^{-/-}$ BMDCs (**Fig. 4a**). Consistent with that finding, the DNA-binding activity of the NF-κB complex containing the p65 subunit was much lower in the nuclei of *Card9*$^{-/-}$ BMDCs after stimulation through ITAM-associated receptors (**Fig. 4b**). In contrast, stimulation of *Card9*$^{+/+}$ and *Card9*$^{-/-}$ BMDCs through FcγR demonstrated no apparent differences in the phosphorylation of the kinases Erk, Jnk and p38 (**Fig. 4a**). These data indicate that CARD9 is essential for the coupling of ITAM receptor signaling to activation of NF-κB but not of MAPK in myeloid cells.

ITAM-mediated myeloid cell activation requires Bcl-10

Because CARD9 interacts with Bcl-10 (ref. 29), we determined whether Bcl-10 functions in the CARD9-dependent, ITAM receptor–mediated activation of myeloid cells. When we stimulated BMDCs from *Bcl10*$^{-/-}$ mice with monoclonal antibodies specific for ITAM receptors or zymosan, cytokine production was substantially impaired, similar to that in *Card9*$^{-/-}$ BMDCs (**Fig. 5a**). Thus, analogous to antigen receptor signaling, Bcl-10 is critically involved in activation signals mediated by means of ITAM-bearing receptors in myeloid cells.

The formation of the complex of Bcl-10 and CARMA1 is essential for antigen receptor signaling in lymphocytes. Splenic DCs and BMDCs have abundantly expression of CARMA1, whereas macrophages have relatively lower expression (**Supplementary Fig. 4** online). Thus, we examined whether CARMA1 also functions in the ITAM receptor–Bcl-10 signaling pathway in myeloid cells. Unlike their responses to TCR and BCR stimulation, *Card11*$^{-/-}$ BMDCs had normal production of TNF and IL-2 after stimulation through FcγR

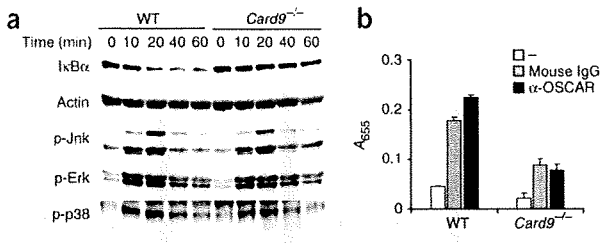

Figure 4 Impaired ITAM-associated receptor–mediated NF-κB activation in *Card9*$^{-/-}$ DCs. **(a)** Immunoblot analysis of lysates of wild-type or *Card9*$^{-/-}$ BMDCs stimulated with anti-CD16 (time, above lanes). p-, phosphorylated. **(b)** DNA-binding assay of NF-κB p65 activity in nuclear extracts from wild-type or *Card9*$^{-/-}$ BMDCs left unstimulated (–) or stimulated for 8 h with immobilized mouse IgG (10 μg/ml) or anti-OSCAR (10 μg/ml). A_{655}, absorbance at 655 nm. Data are the mean ± s.d. of triplicates and are representative of three independent experiments.

(**Fig. 5b**), OSCAR (**Fig. 5c**), TREM-1 (**Fig. 5d**) or zymosan (**Fig. 5e**), suggesting that CARMA1 is not involved in ITAM-mediated myeloid cell activation. These results collectively suggest that the CARD9–Bcl-10 complex but not the CARMA1–Bcl-10 complex relays ITAM-mediated signals for NF-κB activation in myeloid cells.

TLR signaling requires CARD9 and Bcl-10 but not CARMA1

To investigate further the possibility that CARD9 is involved in TLR-MyD88 signaling, we examined the effects of direct stimulation of *Card9*$^{-/-}$ BMDCs with various TLR ligands: Pam_3CSK_4 for TLR2, poly(I:C) for TLR3, LPS for TLR4, flagellin for TLR5, loxoribine for TLR7, and CpG DNA for TLR9. Production of both TNF (**Fig. 6a**) and IL-6 (**Fig. 6b**) was much lower in *Card9*$^{-/-}$ BMDCs than in wild-type BMDCs in response to all TLR ligands tested. In particular, the responses to the TLR7 ligand loxoribine and the TLR3 ligand poly(I:C) were severely impaired in *Card9*$^{-/-}$ BMDCs. Because the induction of *Il6* mRNA after loxoribine stimulation was much lower in *Card9*$^{-/-}$ BMDCs, the impairment in cytokine production seemed to be at the transcriptional level (**Supplementary Fig. 5** online). Notably, like the pattern of impaired cytokine production in response to zymosan stimulation (**Figs. 3b** and **6a–c**), TLR-mediated IL-12 production seemed to be similar in wild-type and *Card9*$^{-/-}$ BMDCs (**Fig. 6c**), suggesting that CARD9 is differentially required for the induction of TNF and/or IL-6 and IL-12. Notably, *Card9*$^{-/-}$ bone marrow–derived macrophages or thioglycolate-induced peritoneal macrophages did not have the defective TLR-induced cytokine production found in DCs (**Supplementary Fig. 6** online), suggesting that the contribution of CARD9 to TLR signaling differs depending on the myeloid cell type. To determine whether Bcl-10 and CARMA1 were involved in the CARD9-mediated TLR signaling pathways in BMDCs, we tested cytokine responses after stimulation with various TLR ligands in *Bcl10*$^{-/-}$ BMDCs and *Card11*$^{-/-}$ BMDCs. As with ITAM receptor signaling, *Bcl10*$^{-/-}$ BMDCs also had defective TLR-induced cytokine production (**Fig. 6d**) but *Card11*$^{-/-}$ BMDCs did not (**Fig. 6e**), suggesting that the CARD9–Bcl-10 complex but not the CARMA1–Bcl-10 complex is involved in TLR signaling.

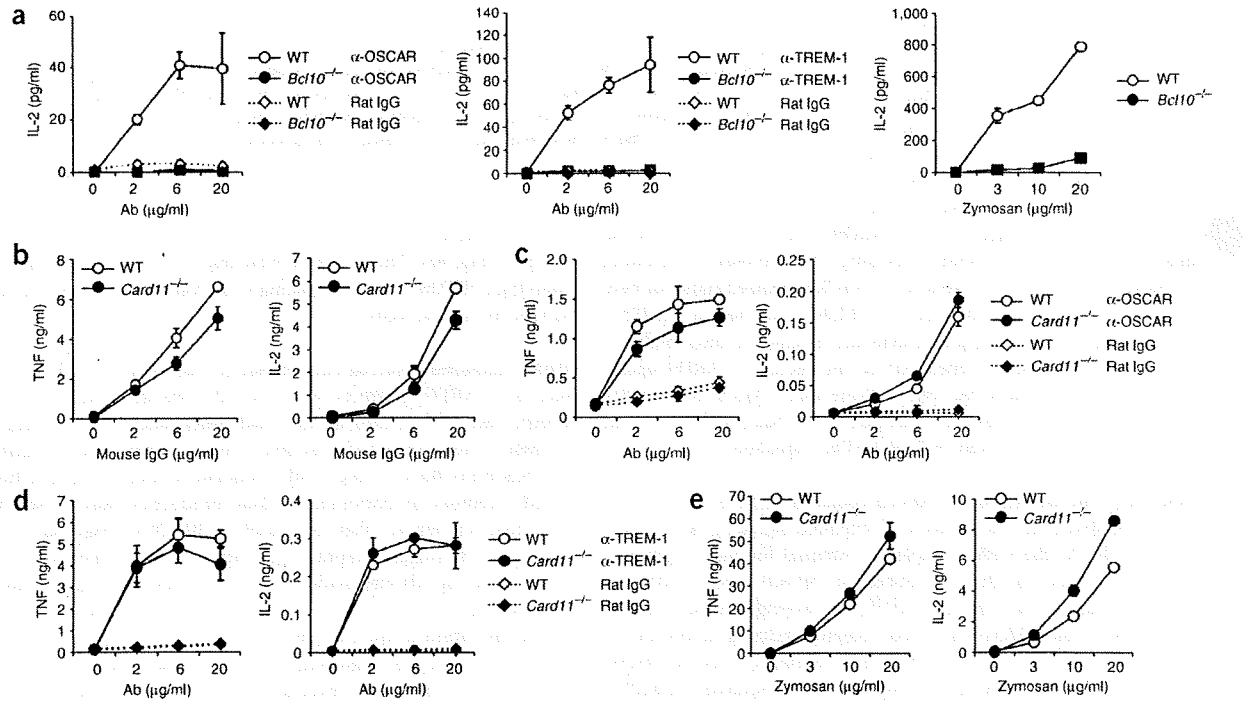

Figure 5 CARD9-dependent ITAM receptor–induced activation of DCs requires Bcl-10 but not CARMA1. **(a)** ELISA of IL-2 production by wild-type or *Bcl10*$^{-/-}$ BMDCs stimulated for 24 h with immobilized monoclonal anti-OSCAR (left) or anti-TREM-1 (middle) or control rat IgG in the presence of FcR blocker (soluble mouse γ-globulin, 10 μg/ml) or stimulated with zymosan (right). **(b–e)** ELISA of the production of TNF and IL-2 by wild-type or *Card11*$^{-/-}$ BMDCs stimulated for 24 h in the presence of FcR blocker with immobilized mouse IgG (**b**), anti-OSCAR (**c**), anti-TREM-1 (**d**) or zymosan (**e**). Rat IgG, control antibody for stimulation (**a,c,d**). Data are the mean ± s.d. of triplicates and are representative of three independent experiments.

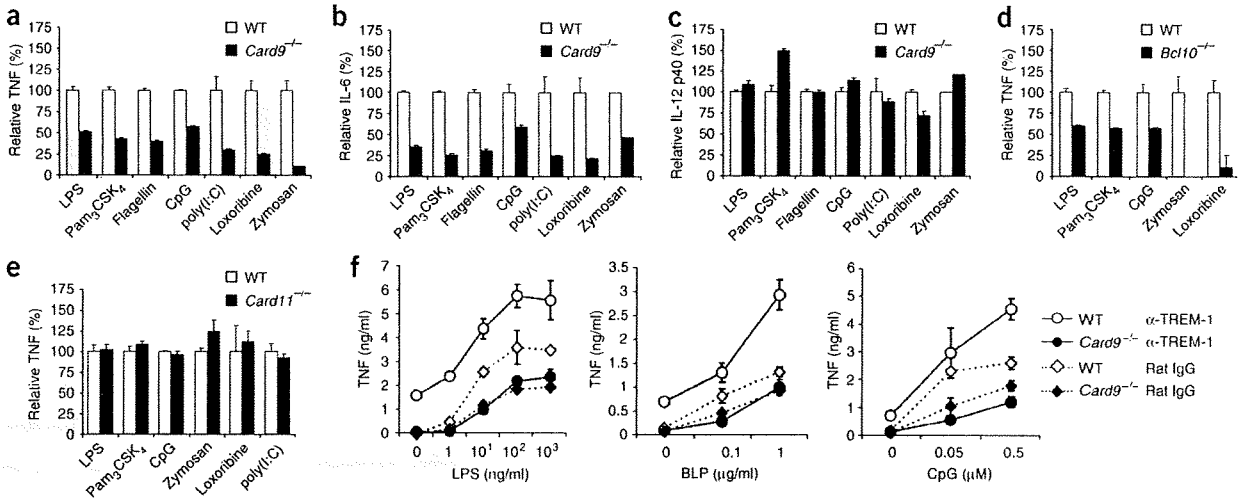

Figure 6 Impaired TLR response by *Card9*$^{-/-}$ DCs. (**a–e**) ELISA of cytokine production by BMDCs stimulated for 24 h with the TLR ligands LPS (100 ng/ml), Pam_3CSK_4 (100 ng/ml), flagellin (100 ng/ml), CpG DNA (1 μM), poly(I:C) (100 μg/ml), loxoribine (100 μM) or zymosan (20 μg/ml; **a–c**) or with all of the TLR ligands in **a–c** except flagellin (**d,e**). Results presented are relative to wild-type production (set at 100%). (**f**) ELISA of TNF production by wild-type or *Card9*$^{-/-}$ BMDCs stimulated with LPS (left), bacterial lipopeptide (BLP; middle) or CpG DNA (right) in the presence of costimulation with immobilized anti-TREM-1 or control rat IgG (10 μg/ml). Data are the mean ± s.d. of triplicates and are representative of six (**a–c**) or two (**d–f**) independent experiments.

TREM-1-mediated TLR responses require CARD9

It has been reported that TREM-1 stimulation augments LPS-induced cytokine responses both *in vitro* and *in vivo*[18]. To determine whether CARD9 is involved in the effect of TREM-1, we stimulated *Card9*$^{-/-}$ BMDCs with TLR ligands, including LPS, Pam_3CSK_4, CpG DNA, in the presence or absence of costimulation with monoclonal anti-TREM-1 and then evaluated TNF production (**Fig. 6f**). TLR-induced TNF production itself without TREM-1 stimulation was much lower in *Card9*$^{-/-}$ BMDCs. Although TNF production after stimulation with TLR ligands was enhanced in the presence of TREM-1 costimulation in wild-type BMDCs, *Card9*$^{-/-}$ BMDCs did not demonstrate such enhancement by TREM-1 costimulation. Thus, these results demonstrate that CARD9 is essential for the augmentation of TLR-mediated cytokine responses by TREM-1.

TLR-mediated MAPK activation requires CARD9

To explore the mechanism of CARD9- and Bcl-10-mediated TLR signaling, we analyzed signaling pathways 'downstream' of TLRs. Because *Card9*$^{-/-}$ BMDCs showed impaired NF-κB activation after stimulation of ITAM-associated receptors (**Fig. 4**), we first examined the activation of NF-κB after TLR stimulation. However, degradation by IκBα (data not shown) and the DNA-binding activity of the p65-containing NF-κB complex were not impaired much in the nuclei of *Card9*$^{-/-}$ BMDCs after stimulation with zymosan (**Fig. 7a**), LPS (**Fig. 7b**) or loxoribine (**Fig. 7c**). In contrast, *Card9*$^{-/-}$ BMDCs had apparent activation defects of the Jnk and p38 MAPKs at early time points after loxoribine stimulation (**Fig. 7d**), and throughout the time course after zymosan stimulation (**Fig. 7e**). These results suggest that CARD9 is involved in signaling for the activation of MAPKs but not of NF-κB in the 'downstream' pathway of TLRs.

A genetic study of mice deficient in the effector molecule RIP2 has shown that RIP2 regulates multiple signaling pathways 'downstream' of TLRs, including p38, Jnk, Erk and IKKs[36]. It has been shown that RIP2 is recruited to the TLR4 receptor complex and associates with the kinase IRAK1 and the adaptor molecule TRAF6 after LPS stimulation[37] and that IRAK1 also recruits Bcl-10 to the TLR4 signaling complex[38]. Moreover, it has been suggested that CARD9 directly associates with the receptor Nod2 and RIP2 and regulates Nod2-mediated activation of p38 and Jnk[39]. Given that the apparent defects in TLR-induced cytokine production by *Card9*$^{-/-}$ and *Bcl10*$^{-/-}$ BMDCs correlated with impaired activation of p38 and Jnk, we hypothesized that CARD9 may function in the signaling pathway mediated by IRAK1–RIP2–Bcl-10.

To determine whether CARD9 physically and functionally associates with RIP2 and/or IRAK1, we expressed these proteins together in HEK293T cells (**Fig. 7f**). There was direct association between RIP2 and IRAK1 (**Fig. 7f**, lane 3) and between RIP2 and Card9 (**Fig. 7f**, lane 4), as reported before[37,39]. When these three molecules were expressed together, they seemed to associate and form a complex (**Fig. 7f**, lane 5). Overexpression of IRAK1 alone did not induce the activation of MAPKs (**Fig. 7f**, lane 1). However, we detected activation of only Jnk (but not p38 and Erk) with the expression of CARD9 or RIP2 alone (**Fig. 7f**, lanes 2 and 3), which was synergistically augmented by the expression of CARD9 and RIP2 together (**Fig. 7f**, lane 4). Expression of the last two molecules together resulted in substantial activation of p38 and weak but notable Erk activation. The Erk activation was enhanced when IRAK1 was expressed together with CARD9 (**Fig. 7f**, lane 5). Notably, the synergistic activation of p38 and Jnk by RIP2 and CARD9 correlated with an increase in the phosphorylated form of Bcl-10 (**Supplementary Fig. 7** online). These collectively results suggest that after TLR stimulation, IRAK1, CARD9 and RIP2 may form a complex and thereby functionally cooperate to activate MAPKs and that Bcl-10 phosphorylation might be involved in regulating that function, which seems to be critical for TLR-induced production of TNF and IL-6 in DCs.

CARD9 is required for antibacterial defense

TLR-mediated responses of macrophages and DCs against bacterial components are crucial for antibacterial defense. It has been

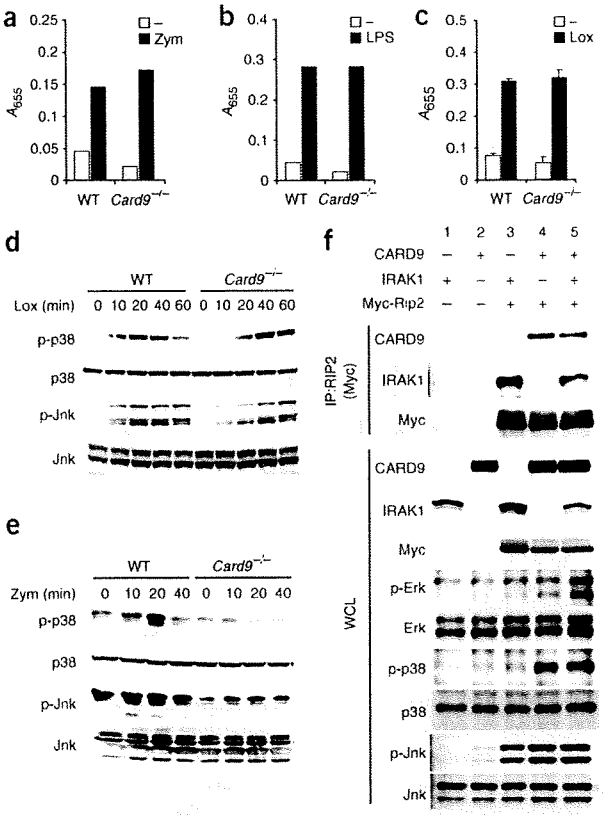

Figure 7 Impaired MAPK activation in TLR-stimulated *Card9*$^{-/-}$ DCs. (**a–c**) DNA-binding activity of NF-κB p65 in nuclear extracts from wild-type or *Card9*$^{-/-}$ BMDCs left unstimulated (–) or stimulated for 2 h with zymosan (Zym; 20 mg/ml; **a**), LPS (1 μg/ml; **b**) or loxoribine (Lox; 100 μM; **c**). (**d,e**) Immunoblot analysis of lysates of wild-type or *Card9*$^{-/-}$ BMDCs stimulated (time, above lanes) with loxoribine (100 μM; **d**) or zymosan (20 μg/ml; **e**). (**f**) Immunoblot analysis of HEK293T cells transfected with 0.5 μg of various combinations (above lanes) of expression plasmids encoding IRAK1, CARD9 or Myc-tagged RIP2; at 30 h after transfection, cell lysates were immunoprecipitated with anti-Myc and then the immunoprecipitates (IP) and lysates (WCL) were analyzed with antibodies specific for various proteins (left margin). Data are the mean + s.d. of two experiments (**a-c**) or are representative of two experiments (**d–f**).

demonstrated that TLR-mediated, MyD88-dependent signaling is essential for control of *Listeria monocytogenes* infection[40,41]. To examine the *in vivo* effect of CARD9 deficiency, we infected wild-type and *Card9*$^{-/-}$ mice with *L. monocytogenes* and then analyzed the bacterial burden of the infected organs at 3 d after the infection. We detected a significantly higher listerial burden in the infected spleens and livers of *Card9*$^{-/-}$ mice than in those from wild-type mice (**Fig. 8**), indicating that *Card9*$^{-/-}$ mice are more susceptible to *L. monocytogenes* infection than are wild-type mice. These *in vivo* results demonstrate that CARD9 is crucial for antibacterial defense, presumably through TLRs and their costimulating ITAM receptors. Our results collectively demonstrate that the activation of lymphoid and myeloid cells through ITAM receptors and TLRs are mediated by two different types of complexes containing Bcl-10–MALT1: lymphoid type (CARMA1–Bcl-10–MALT1) and myeloid type (CARD9–Bcl-10–MALT1), respectively (**Supplementary Fig. 8** online).

DISCUSSION

In vitro studies and *in vivo* genetic analyses of deficient mice have shown that the CBM complex, composed of CARMA1, Bcl-10 and MALT1, is essential for TCR- and BCR-mediated NF-κB activation. In addition, the CBM complex is involved in TLR4 and CD40 signaling in B cells[22,23,26,28]. As CARD9 was originally identified as a protein that interacts with Bcl-10 through its CARD and triggers NF-κB activation in a synergistic way with Bcl-10, we hypothesized that CARD9 could function in antigen receptor, TLR and/or CD40 signaling by interacting with Bcl-10. However, our results here have shown that CARD9 is dispensable for those receptor-mediated lymphocyte activation responses. That might be due in part to the lower expression of CARD9 in lymphoid cells than in myeloid cells.

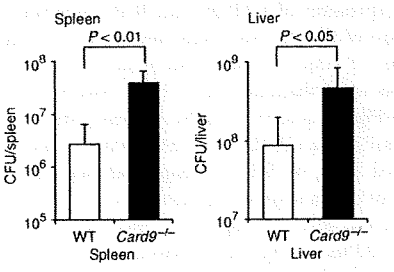

Figure 8 *Card9*$^{-/-}$ mice are more susceptible to *L. monocytogenes*. Quantification of colony-forming units (CFU) of *L. monocytogenes* in the spleens (left) and livers (right) of wild-type and *Card9*$^{-/-}$ mice infected intraperitoneally for 3 d with 5×10^5 *L. monocytogenes*. Data are the means + s.d. of groups of seven mice and are representative of two independent experiments.

Alternatively, perhaps it can be attributed to the structure of CARD9: whereas CARD9 is similar to CARMA1 in terms of the highly homologous CARD and the flanking coiled-coil domain at its amino terminus, CARMA1 but not CARD9 has the carboxy-terminal MAGUK 'signature' domains (PDZ, SH3 and Guk) required for CARMA1 signaling function[42,43]. In addition, the 'linker' region that connects the coiled-coil and PDZ domains of CARMA1 is short in CARD9 (ref. 29) and thus lacks the PKC phosphorylation sites that are critical for TCR- or BCR-mediated NF-κB activation[44,45]. Therefore, CARD9 might be incapable of coupling receptor-induced PKC activation to 'downstream' NF-κB activation despite having a Bcl-10-interacting CARD. Indeed, our data have confirmed that CARD9 deficiency did not affect DC activation induced by the direct PKC activator phorbol 12-myristate 13-acetate plus ionomycin. The unique structural characteristics of CARMA1 may generate the specificity of Bcl-10–MALT1–mediated NF-κB activation in antigen receptor signaling.

It has been established that Bcl-10–MALT1–mediated signaling is essential for NF-κB activation by TCRs and BCRs in lymphocytes and by FcεRI in mast cells. All of those receptors deliver signals by associating with signaling adaptors containing ITAMs. Our data now extend that knowledge regarding lymphocyte signaling to myeloid cells by demonstrating that Bcl-10 is also essential for NF-κB activation through various ITAM receptors expressed on myeloid cells. Our results collectively indicate a general principle that a Bcl-10–MALT1–containing complex is an essential mediator of NF-κB activation through ITAM receptors in immune cells.

Based on analyses of the function of the CBM complex in antigen receptor signaling, we assumed that the formation of a complex of

Bcl-10–MALT1 with CARMA1 would be a prerequisite for 'downstream' IKK activation even in myeloid cells. However, we found that CARMA1 was dispensable for Bcl-10-mediated ITAM receptor signaling in myeloid cells and instead found that CARD9 was the essential molecule mediating this pathway. Thus, we propose that the CARD9–Bcl10–MALT1 complex is responsible for mediating ITAM receptor signaling in myeloid cells and we further stipulate that the classical CBM (CARMA1–Bcl-10–MALT1) complex is the lymphoid complex, whereas the newly identified CARD9–Bcl-10–MALT1 complex is the myeloid complex.

The production of TNF, IL-2, IL-6 and IL-12 after the stimulation of FcRγ- or DAP12-associated receptors, including FcγR, OSCAR, TREM-1 and MAIR-II, was impaired in *Card9*$^{-/-}$ BMDCs, indicating a critical function for the myeloid CARD9–Bcl-10–MALT1 complex in ITAM-associated receptor–mediated cytokine expression. However, IL-12 production mediated by the ITAM-bearing receptor dectin-1 in response to zymosan was not affected by CARD9 deficiency, although the production of IL-2, IL-6 and TNF was impaired. Because zymosan has been shown to stimulate both the dectin-1–Syk and TLR-MyD88 signaling pathways for cytokine production, we examined in which of those pathways CARD9 is involved; to do this we simultaneously analyzed DCs from *Card9*$^{-/-}$, *Myd88*$^{-/-}$ and *Clec7a*$^{-/-}$ mice. We found that, consistent with published reports[31,32], zymosan-induced cytokine production depended mainly on the TLR-MyD88 but not the dectin-1–Syk pathway. However, stimulation of DCs from these knockout mice with NaClO-oxidized zymosan, a purified β-glucan agent that does not activate the TLR-MyD88 pathway, showed that CARD9 was essential for the production of cytokines, including IL-12, by dectin-1 signaling . Our data collectively establish the idea that CARD9 generally functions 'downstream' of ITAM-bearing adaptors and receptors and is essential for the induction of all cytokine expression by regulating NF-κB activation in myeloid cells. The data showing that CARD9 functions in the TLR-MyD88 pathway also led us to consider that CARD9 is involved in general TLR-MyD88 signaling.

Studies have shown that Bcl-10 is involved in TLR4 signaling in B cells[28] and that the RNA interference–mediated depletion of Bcl-10 in a macrophage cell line results in the impairment of LPS-induced NF-κB activation *in vitro*[46]. Our results have provided genetic evidence that Bcl-10 is involved in various other TLR signaling pathways in addition to TLR4 signaling in DCs. CARMA1 is also involved in TLR4 signaling in B cells by regulating Jnk activation[22,23,26,28]. Although DCs and B cells have similarly high expression of CARMA1, we found that CARMA1 deficiency did not affect TLR signaling in DCs, but instead that the Bcl-10-mediated TLR pathway was controlled by CARD9, similar to ITAM receptor signaling. Those findings indicate that the myeloid CARD9–Bcl-10–MALT1 complex functions not only in ITAM receptor–mediated signaling pathways but also in TLR-signaling pathways in DCs.

However, we also found that 'downstream' signaling events controlled by the myeloid CARD9–Bcl-10–MALT1 complex were different for ITAM receptors and TLRs. Whereas the myeloid CARD9–Bcl-10–MALT1 complex controlled the activation of NF-κB but not MAPKs in ITAM-receptor signaling, in TLR signaling it controlled the activation of MAPKs but not NF-κB. Although zymosan-induced activation of p38 and Jnk was lower in *Card9*$^{-/-}$ mice, loxoribine-induced activation of these kinases were not impaired much, which correlated with delayed onset of activation. Such an activation delay might affect proper induction of cytokine genes, as *Myd88*$^{-/-}$ macrophages, which show signaling abnormality only with delayed activation of NF-κB and MAPKs in response to LPS, have an almost complete lack of cytokine production[47].

Our finding that *Card9*$^{-/-}$ BMDCs had impaired production of TNF and IL-6 but not of IL-12 led to our model that two different pathways operate 'downstream' of TLRs in DCs: the myeloid CARD9–Bcl-10–MALT1 complex–dependent pathway we have outlined here, which contributes mainly to IL-6 and TNF gene expression through MAPK activation; and a distinct myeloid CARD9–Bcl-10–MALT1 complex–independent pathway, which probably depends on MyD88 and/or the adaptor TRIF[48]. The latter pathway may trigger *Il12* expression through NF-κB activation but is not enough to induce TNF and IL-6 production. Similar signal dependency for the expression of a different set of cytokine genes has been reported for CD40 signaling in DCs[49]. After CD40 stimulation, activation of NF-κB but not p38 is required for IL-12 production, whereas activation of p38 but not NF-κB is required for IL-6 production. These data suggest that there is epigenetically differential regulation of TNF and IL-6 versus IL-12 through the use of MAPK or NF-κB activation.

Our *in vitro* overexpression study suggested that the signaling pathway dependent on the myeloid CARD9–Bcl-10–MALT1 complex seems to be mediated by IRAK1- and RIP2-mediated Bcl-10 phosphorylation and that it induces 'downstream' MAPK activation. Support for the idea of a functional IRAK1–RIP2–CARD9–Bcl-10–dependent pathway is found in the similar phenotypes of mice deficient in CARD9 or RIP2, in which myeloid cells are hyporesponsive to various TLR stimuli[36] and hence the mice become susceptible to *L. monocytogenes* infection[50]. The finding that *Card9*$^{-/-}$ DCs had impaired cytokine responses to stimulation by a variety of MyD88-mediated TLR ligands may be explained by the molecular 'linkage' of IRAK1 and CARD9, as IRAK1 is recruited to the TLR complex through MyD88–adaptor molecule TIRAP after TLR stimulation, after which IRAK1 associates with TRAF6 to further activate 'downstream' IKK complexes and MAPKs[38]. Our data have shown that *Card9*$^{-/-}$ BMDCs had impaired cytokine response after stimulation with poly(I:C), a ligand for TLR3 that transduces signals by association with TRIF independently of MyD88. It has been reported that *Card9*$^{-/-}$ macrophages have impaired MAPK activation in response to *in vitro* infection by the double-stranded RNA virus vascular stomatitis virus, suggesting that CARD9 controls signaling through RIG-I, which senses intracellular double-stranded RNA[51]. Thus, the impaired cytokine response to poly(I:C) in *Card9*$^{-/-}$ BMDCs might be attributed to impairment of RIG-I-mediated signaling. Alternatively, a common 'downstream' molecule may couple both MyD88-mediated and TRIF-mediated signaling to CARD9-regulated MAPK activation. However, the exact molecular connection leading to MAPK activation 'downstream' of CARD9 remains to be addressed.

The finding that DCs but not macrophages from *Card9*$^{-/-}$ mice had impaired TLR signaling suggests that cytokine production mediated by the myeloid CARD9–Bcl-10–MALT1 complex is induced in a cell type–specific way. Similar cell type specificity of pattern-recognition receptor signaling has been reported for RIG-I-mediated production of type I interferon[52]. The exact mechanistic basis for the function of the myeloid CARD9–Bcl-10–MALT1 complex 'downstream' of specific TLRs in DCs remains to be determined.

In conclusion, we have shown here that the CARD9–Bcl-10 complex was critical for ITAM receptor–mediated myeloid cell activation and was also required for TLR-induced cytokine responses in DCs. In contrast, CARMA1 was dispensable for those receptor-mediated myeloid cell activation responses. Our results have provided genetic evidence of essential and nonredundant functions for the CBM complex in lymphoid cells and the CARD9–Bcl-10–MALT1 complex in myeloid cells in the ITAM receptor–mediated and TLR-mediated cellular activation and immune responses. Based on our findings,

therapeutic approaches targeting either the lymphoid CBM complex or the myeloid CARD9–Bcl-10–MALT1 complex might provide a strategy for specifically modulating lymphoid versus myeloid cells for the activation or inhibition of their functional responses.

METHODS

Mice and gene targeting of *Card9*. *Card11*$^{-/-}$, *Bcl10*$^{-/-}$, *Myd88*$^{-/-}$ and *Clec7a*$^{-/-}$ mice were generated before[26,28,47]. C57BL/6 and BALB/c mice were from Clea Japan. All mice were maintained at the animal facility of the RIKEN Research Center for Allergy and Immunology according to institutional guidelines.

Card9 was isolated from genomic DNA extracted from embryonic stem cells (R1) by PCR. The targeting vector was constructed by replacement of exon 2, including the ATG start codon and the CARD-encoding region, with a neomycin-resistance gene cassette, and insertion of a fragment of the gene encoding diphtheria toxin A driven by the phosphoglycerate kinase promoter into the genomic fragment (for negative selection). After the targeting vector was transfected into embryonic stem cells, G418-resistant colonies were selected, screened by PCR and further confirmed by Southern blot analysis. Germline chimeras were generated by aggregation. The resulting male chimeras were backcrossed with C57BL/6J females, and germline transmission in F_1 *Card9*$^{+/-}$ mice was verified by Southern blot analysis. *Card9*$^{+/-}$ mice that were backcrossed for at least five generations with C57BL/6J mice were intercrossed to obtain *Card9*$^{-/-}$ mice with the C57BL/6 genetic background. *Card9*$^{-/-}$ and C57BL/6J control (wild-type) mice were used throughout the experiments.

Antibodies, transfection, plasmids and reagents. Antibodies specific for MAIR-II (ref. 14) and OSCAR[53] have been described. Antibodies specific for Erk (9102), phosphorylated Erk (9101), p38 (9212), phosphorylated p38 (9102), Jnk (9258), phosphorylated Jnk (9251) and IκBα (9242) were from Cell Signaling Technology; anti-actin (sc-8432), anti-c-Myc (sc-789), anti-IRAK1 (sc-7883) and anti-Bcl-10 (331.3) were from Santa Cruz Biotechnology; anti-RIP2 (PX092) was from Cell Science; anti-TREM-1 (174031) was from R&D Systems; anti-CD40 (3/23) and anti-CD16 (2.4G2) were from BD Bioscience; and anti-Flag (M2) was from Sigma. The expression plasmid pCMV-flag–Card9 was created by PCR. Expression plasmids encoding IRAK-1 (pCMV-SPORT–IRAK1), CARD9 (pCMV-Flag–Card9), and Myc-tagged RIP2 (pcDNA3-Myc–RIP2) were also used. Rabbit anti-CARD9 serum was raised against a synthetic peptide corresponding to amino acids 520–536 of mouse CARD9 (CGDRGNTTGSDNTDTEGS). Zymosan, LPS and poly(I:C) (polyinosinic-polycytidylic acid) were from Sigma; phosphorothioate-stabilized CpG DNA (ODN 1668; TCCATGACGTTCCTGATGCT) was from Hokkaido System Science; and Pam_3CSK_4 (*N*-palmitoyl-*S*-[2,3-bis(palmitoyloxy)-(2*RS*)-propyl]-[*R*]-Cys-[*S*]-Ser$_3$-[*S*]-Lys4 trihydrochloride), flagellin, loxoribine, R837 (imiquimod), R848 (resiquimod) and zymosan were from Invivogen. NaClO-oxidized zymosan was prepared as described[35].

For transfection, HEK293T cells (1×10^5) were plated on 24-well culture dishes and were transfected with expression plasmids by lipofection with Lipofectamine LTX according to the manufacturer's instructions (Invitrogen). Lysates of transfected cells were separated by SDS-PAGE at 30 h after transfection and then exogeneously expressed and endogeneous proteins were analyzed by immunoblot.

Cell preparation and flow cytometry. Whole T cells from lymph nodes or spleen were purified by magnetic-activated cell sorting (MACS; Miltenyi Biotec) for removal of B220$^+$, NK1.1$^+$, Mac-1$^+$ and Gr-1$^+$ cells; the purity was over 95% CD3$^+$ by flow cytometry. CD4$^+$ or CD8$^+$ T cells were isolated from purified whole T cell samples by positive sorting with MACS. Splenic B cells were purified by MACS for the removal of CD3$^+$, NK1.1$^+$, Mac-1$^+$ and Gr-1$^+$ cells; the purity was over 95% B220$^+$ by flow cytometry. BMDCs or bone marrow–derived macrophages were prepared by culture of bone marrow cells for 5–10 d with granulocyte-macrophage colony-stimulating factor (20 ng/ml; Peprotech) or for 3–5 d with macrophage colony-stimulating factor (25 ng/ml; Peprotech), respectively. Thioglycolate-induced peritoneal macrophages were prepared as described[32].

For flow cytometry, single-cell suspensions of thymus, lymph node, bone marrow and spleen were stained with fluorescein isothiocyanate–, phycoerythrin-, allophycocyanin- or biotin-conjugated antibodies. Biotinylated antibodies were visualized with streptavidin–peridinine chlorophyll protein (BD Pharmingen). Antibodies used were to B220, IgM, IgD, CD21, CD23, CD4, CD8, CD3, CD25, CD44 and CD69. Stained cells were analyzed with a FACSCalibur (Becton Dickinson) and CellQuest software (BD Biosciences).

Immunoassays, real-time PCR and NF-κB DNA binding. BMDCs were stimulated with anti-CD16 (2.4G2; Pharmingen) followed by crosslinking with anti–rat IgG F(ab′)$_2$ (112-006-072; Jackson ImmunoResearch) or with 100 μM loxoribine (Invivogen). After incubation at 37 °C for various periods of time, cells were lysed in ice-cold lysis buffer (50 mM Tris-HCl, pH 8.0, 150 mM NaCl, 1.0% (vol/vol) Triton X-100, 20 mM EDTA, 1 mM Na_3VO_4, 1 mM NaF and protease inhibitors). Cell lysates were separated by SDS-PAGE and proteins were transferred onto polyvinyldifluoride membranes. Membranes were incubated with antibodies to Erk, phosphorylated Erk, p38, phosphorylated p-38, Jnk, phosphorylated Jnk, IκBα, actin, c-Myc, Flag and Bcl-10 and then with horseradish peroxidase–conjugated secondary antibodies, followed by development with the ECL detection system (Amersham Pharmacia). Band intensities were quantified with a LAS-3000 imaging system (FUJIFILM).

For real-time PCR, total RNA was extracted from cells with TRIzol reagent (Invitrogen). For cDNA synthesis, total RNA was reverse-transcribed with SuperScript II and random hexamers according to the manufacturer's instructions (Life Technologies). The cDNA was analyzed quantitatively for expression of genes with the quantitative PCR system iCycler (BIO-RAD). Primer sequences were as follows: mouse *Card9*, forward, 5′-CCCGATGATGAGGAG CAG-3′, and reverse, 5′-AAGCCACGTAGCCCTTGT-3′; and *Il6* forward, 5′-ACAACCACGGCCTTCCCTACTT-3′, and reverse, 5′-CACGATTTCCCAGA GAACATGTG-3′.

For analysis of NF-κB activity, BMDCs were stimulated for 8 h with immobilized anti-OSCAR (10 μg/ml), mouse γ-globulin (10 μg/ml) or LPS (1 μg/ml). Nuclear extracts were prepared from the stimulated cells and the binding activity of NF-κB subunit p65 in the extracts was measured with a Mercury TransFactor kit (Clontech).

***In vitro* functional analyses of T cells, B cells, DCs and macrophages.** For proliferation assays, T cells were stimulated with anti-CD3ε (145-2C11; Pharmingen), anti-CD28 (37.51; Pharmingen), phorbol 12-myristate 13-acetate (10 ng/ml) plus ionomycin (1 μM), and staphylococcal enterotoxin B (5–500 ng/ml; SC BioScience) together with irradiated syngeneic spleen cells. Purified B cells were stimulated with anti-IgM F(ab′)$_2$ (115-006-020; Jackson ImmunoResearch), anti-CD40, recombinant mouse IL-4 (R&D Systems), LPS and CpG DNA. After 2 or 3 d, cultures were pulsed for 8 h with 1 μCi [^{3}H]thymidine (Amersham) and collected. [^{3}H]thymidine incorporation was measured with a Microbeta (Perkin-Elmer) or Matrix 96 (Packard). For cytokine production assays, supernatants of CD4$^+$ and CD8$^+$ T cells were assayed in triplicate by ELISA (R&D Systems) for IFN-γ production. For allogenic T cell responses, purified T cells (5×10^4) from C57BL/6 mice were cultured for 48 h with irradiated (30 Gy) spleen cells (2.5×10^5) from BALB/c mice and [^{3}H]thymidine incorporation was measured in a similar way.

BMDCs or macrophages were stimulated with immobilized anti-CD16, anti-TREM-1, anti-OSCAR, anti-MAIR-II or isotype control rat IgG in the presence of soluble mouse γ-globulin (10 μg/ml) as an FcR blocker or with zymosan. IL-2, TNF, IL-6 and IL-12 in culture supernatants were analyzed with ELISA kits (BD Bioscience).

***In vivo* antibody responses.** Mice were immunized intraperitoneally with 100 μg DNP-KLH (LSL) adsorbed to alum (Sigma). At 24 d after immunization, DNP-specific serum titers were determined by ELISA (Southern Biotechnology Associates) in plates coated with DNP–human serum albumin (LSL).

Listeria infection. *L. monocytogenes* strain EGD was used. C57BL/6 mice were infected intraperitoneally with one fifth of the 50% lethal dose (5×10^5 colony-forming units per mouse) of *L. monocytogenes* in 0.2 ml of PBS. Bacterial burdens in the spleen and liver were determined 3 d after infection by plating of tenfold serial dilutions of organ homogenates on tryptic soy agar plates. Colonies

were counted after 24 h of incubation at 37 °C. Experiments were done according to institutional guidelines and were approved by institutional committees.

Note: Supplementary information is available on the Nature Immunology website.

ACKNOWLEDGMENTS

We thank N. Suzuki, S. Yamasaki, and T. Yokosuka for discussions; H. Arase (Osaka University) and N. Kanazawa (Wakayama Medical University) for reagents; S. Akira (Osaka University) for *Myd88*$^{-/-}$ mice and *Tlr2*$^{-/-}$; X. Lin (University of Texas M.D. Anderson Cancer Center) for reagents, discussions and sharing unpublished data; and H. Yamaguchi and M. Ikari for secretarial assistance. Expression plasmids pCMVSPORT-IRAK1, pcDNA3-RIP2–myc and pRK6–myc-Bcl-10 were provided by T.W. Mak (Campbell Family Institute for Breast Cancer Research and Ontario Cancer Institue), N. Inohara (The University of Michigan Medical School) and X. Lin (University of Texas M.D. Anderson Cancer Center), respectively. Supported by a Grant-in-Aid for Priority Area Research from the Ministry of Education, Culture, Sports, Science and Technology of Japan, the National Cancer Institute (R01 CA87064 to S.W.M.), Cancer Center (CORE grant CA21765), the Council of Scientific and Industrial Research (Government of India; S.K.P.), the Department of Biotechnology (Government of India) and the American Lebanese Syrian Associated Charities of St. Jude Children's Research Hospital.

AUTHOR CONTRIBUTIONS

H.H. designed and did experiments and wrote the paper; C.I., A.T. and H.K. made knockout mice; T.I. did experiments; L.X., S.W.M., S.S. and Y.I. provided knockout mice; M.I., T.T., A.S. and N.O. provided antibodies or reagents; H.Y. and J.M.P. contributed to discussions; and T.S. designed experiments and wrote the paper.

COMPETING INTERESTS STATEMENT

The authors declare no competing financial interests.

Published online at http://www.nature.com/natureimmunology/
Reprints and permissions information is available online at http://npg.nature.com/reprintsandpermissions

1. DeFranco, A.L. Transmembrane signaling by antigen receptors of B and T lymphocytes. *Curr. Opin. Cell Biol.* **7**, 163–175 (1995).
2. Humphrey, M.B., Lanier, L.L. & Nakamura, M.C. Role of ITAM-containing adapter proteins and their receptors in the immune system and bone. *Immunol. Rev.* **208**, 50–65 (2005).
3. Maeda, A., Kurosaki, M. & Kurosaki, T. Paired immunoglobulin-like receptor (PIR)-A is involved in activating mast cells through its association with Fc receptor γ chain. *J. Exp. Med.* **188**, 991–995 (1998).
4. Ono, M., Yuasa, T., Ra, C. & Takai, T. Stimulatory function of paired immunoglobulin-like receptor-A in mast cell line by associating with subunits common to Fc receptors. *J. Biol. Chem.* **274**, 30288–30296 (1999).
5. Lopez-Botet, M. *et al.* Paired inhibitory and triggering NK cell receptors for HLA class I molecules. *Hum. Immunol.* **61**, 7–17 (2000).
6. Kanazawa, N., Tashiro, K., Inaba, K. & Miyachi, Y. Dendritic cell immunoactivating receptor, a novel C-type lectin immunoreceptor, acts as an activating receptor through association with Fc receptor γ chain. *J. Biol. Chem.* **278**, 32645–32652 (2003).
7. Merck, E. *et al.* OSCAR is an FcRγ-associated receptor that is expressed by myeloid cells and is involved in antigen presentation and activation of human dendritic cells. *Blood* **104**, 1386–1395 (2004).
8. Colonna, M. TREMs in the immune system and beyond. *Nat. Rev. Immunol.* **3**, 445–453 (2003).
9. Bakker, A.B., Baker, E., Sutherland, G.R., Phillips, J.H. & Lanier, L.L. Myeloid DAP12-associating lectin (MDL)-1 is a cell surface receptor involved in the activation of myeloid cells. *Proc. Natl. Acad. Sci. USA* **96**, 9792–9796 (1999).
10. Tomasello, E. *et al.* Association of signal-regulatory proteins β with KARAP/DAP-12. *Eur. J. Immunol.* **30**, 2147–2156 (2000).
11. Shiratori, I., Ogasawara, K., Saito, T., Lanier, L.L. & Arase, H. Activation of natural killer cells and dendritic cells upon recognition of a novel CD99-like ligand by paired immunoglobulin-like type 2 receptor. *J. Exp. Med.* **199**, 525–533 (2004).
12. Aguilar, H. *et al.* Molecular characterization of a novel immune receptor restricted to the monocytic lineage. *J. Immunol.* **173**, 6703–6711 (2004).
13. Wright, G.J. *et al.* Characterization of the CD200 receptor family in mice and humans and their interactions with CD200. *J. Immunol.* **171**, 3034–3046 (2003).
14. Yotsumoto, K. *et al.* Paired activating and inhibitory immunoglobulin-like receptors, MAIR-I and MAIR-II, regulate mast cell and macrophage activation. *J. Exp. Med.* **198**, 223–233 (2003).
15. Daeron, M. Fc receptor biology. *Annu. Rev. Immunol.* **15**, 203–234 (1997).
16. Merck, E. *et al.* Fc receptor γ-chain activation via hOSCAR induces survival and maturation of dendritic cells and modulates Toll-like receptor responses. *Blood* **105**, 3623–3632 (2005).
17. Klesney-Tait, J., Turnbull, I.R. & Colonna, M. The TREM receptor family and signal integration. *Nat. Immunol.* **7**, 1266–1273 (2006).
18. Bouchon, A., Facchetti, F., Weigand, M.A. & Colonna, M. TREM-1 amplifies inflammation and is a crucial mediator of septic shock. *Nature* **410**, 1103–1107 (2001).
19. Brown, G.D. Dectin-1: a signalling non-TLR pattern-recognition receptor. *Nat. Rev. Immunol.* **6**, 33–43 (2006).
20. Young, S.H., Ye, J., Frazer, D.G., Shi, X. & Castranova, V. Molecular mechanism of tumor necrosis factor-α production in 1→3-β-glucan (zymosan)-activated macrophages. *J. Biol. Chem.* **276**, 20781–20787 (2001).
21. Rogers, N.C. *et al.* Syk-dependent cytokine induction by dectin-1 reveals a novel pattern recognition pathway for C type lectins. *Immunity* **22**, 507–517 (2005).
22. Ruland, J. *et al.* Bcl10 is a positive regulator of antigen receptor-induced activation of NF-κB and neural tube closure. *Cell* **104**, 33–42 (2001).
23. Ruefli-Brasse, A.A., French, D.M. & Dixit, V.M. Regulation of NF-κB-dependent lymphocyte activation and development by paracaspase. *Science* **302**, 1581–1584 (2003).
24. Ruland, J., Duncan, G.S., Wakeham, A. & Mak, T.W. Differential requirement for Malt1 in T and B cell antigen receptor signaling. *Immunity* **19**, 749–758 (2003).
25. Klemm, S. *et al.* The Bcl10-Malt1 complex segregates Fc epsilon RI-mediated nuclear factor κB activation and cytokine production from mast cell degranulation. *J. Exp. Med.* **203**, 337–347 (2006).
26. Hara, H. *et al.* The MAGUK family protein CARD11 is essential for lymphocyte activation. *Immunity* **18**, 763–775 (2003).
27. Hara, H. *et al.* The molecular adapter Carma1 controls entry of IκB kinase into the central immune synapse. *J. Exp. Med.* **200**, 1167–1177 (2004).
28. Xue, L. *et al.* Defective development and function of Bcl10-deficient follicular, marginal zone and B1 B cells. *Nat. Immunol.* **4**, 857–865 (2003).
29. Bertin, J. *et al.* CARD9 is a novel caspase recruitment domain-containing protein that interacts with BCL10/CLAP and activates NF-κB. *J. Biol. Chem.* **275**, 41082–41086 (2000).
30. Gross, O. *et al.* Card9 controls a non-TLR signalling pathway for innate anti-fungal immunity. *Nature* **442**, 651–656 (2006).
31. Gantner, B.N., Simmons, R.M., Canavera, S.J., Akira, S. & Underhill, D.M. Collaborative induction of inflammatory responses by dectin-1 and Toll-like receptor 2. *J. Exp. Med.* **197**, 1107–1117 (2003).
32. Saijo, S. *et al.* Dectin-1 is required for host defense against *Pneumocystis carinii* but not against *Candida albicans*. *Nat. Immunol.* **8**, 39–46 (2007).
33. Underhill, D.M. *et al.* The Toll-like receptor 2 is recruited to macrophage phagosomes and discriminates between pathogens. *Nature* **401**, 811–815 (1999).
34. Ozinsky, A. *et al.* The repertoire for pattern recognition of pathogens by the innate immune system is defined by cooperation between Toll-like receptors. *Proc. Natl. Acad. Sci. USA* **97**, 13766–13771 (2000).
35. Hida, S., Nagi-Miura, N., Adachi, Y. & Ohno, N. Beta-glucan derived from zymosan acts as an adjuvant for collagen-induced arthritis. *Microbiol. Immunol.* **50**, 453–461 (2006).
36. Kobayashi, K. *et al.* RICK/Rip2/CARDIAK mediates signalling for receptors of the innate and adaptive immune systems. *Nature* **416**, 194–199 (2002).
37. Lu, C. *et al.* Participation of Rip2 in lipopolysaccharide signaling is independent of its kinase activity. *J. Biol. Chem.* **280**, 16278–16283 (2005).
38. Dong, W. *et al.* The IRAK-1–BCL10-MALT1-TRAF6–TAK1 cascade mediates signaling to NF-κB from Toll-like receptor 4. *J. Biol. Chem.* **281**, 26029–26040 (2006).
39. Hsu, Y.M. *et al.* The adaptor protein CARD9 is required for innate immune responses to intracellular pathogens. *Nat. Immunol.* **8**, 198–205 (2007).
40. Seki, E. *et al.* Critical roles of myeloid differentiation factor 88-dependent proinflammatory cytokine release in early phase clearance of *Listeria monocytogenes* in mice. *J. Immunol.* **169**, 3863–3868 (2002).
41. Torres, D. *et al.* Toll-like receptor 2 is required for optimal control of *Listeria monocytogenes* infection. *Infect. Immun.* **72**, 2131–2139 (2004).
42. Wang, D. *et al.* CD3/CD28 costimulation-induced NF-κB activation is mediated by recruitment of protein kinase C-θ, Bcl10, and IκB kinase β to the immunological synapse through CARMA1. *Mol. Cell. Biol.* **24**, 164–171 (2004).
43. Pomerantz, J.L., Denny, E.M. & Baltimore, D. CARD11 mediates factor-specific activation of NF-κB by the T cell receptor complex. *EMBO J.* **21**, 5184–5194 (2002).
44. Sommer, K. *et al.* Phosphorylation of the CARMA1 linker controls NF-κB activation. *Immunity* **23**, 561–574 (2005).
45. Matsumoto, R. *et al.* Phosphorylation of CARMA1 plays a critical role in T Cell receptor-mediated NF-κB activation. *Immunity* **23**, 575–585 (2005).
46. Liu, Y. *et al.* BCL10 mediates lipopolysaccharide/toll-like receptor-4 signaling through interaction with Pellino2. *J. Biol. Chem.* **279**, 37436–37444 (2004).
47. Kawai, T., Adachi, O., Ogawa, T., Takeda, K. & Akira, S. Unresponsiveness of MyD88-deficient mice to endotoxin. *Immunity* **11**, 115–122 (1999).
48. Yamamoto, M., Takeda, K. & Akira, S. TIR domain-containing adaptors define the specificity of TLR signaling. *Mol. Immunol.* **40**, 861–868 (2004).
49. Yanagawa, Y. & Onoe, K. Distinct regulation of CD40-mediated interleukin-6 and interleukin-12 productions via mitogen-activated protein kinase and nuclear factor κB-inducing kinase in mature dendritic cells. *Immunology* **117**, 526–535 (2006).
50. Chin, A.I. *et al.* Involvement of receptor-interacting protein 2 in innate and adaptive immune responses. *Nature* **416**, 190–194 (2002).
51. Yoneyama, M. *et al.* The RNA helicase RIG-I has an essential function in double-stranded RNA-induced innate antiviral responses. *Nat. Immunol.* **5**, 730–737 (2004).
52. Kato, H. *et al.* Cell type-specific involvement of RIG-I in antiviral response. *Immunity* **23**, 19–28 (2005).
53. Koga, T. *et al.* Costimulatory signals mediated by the ITAM motif cooperate with RANKL for bone homeostasis. *Nature* **428**, 758–763 (2004).

Cell Death and Differentiation (2007) 14, 1475–1485

www.nature.com/cdd

Aberrant quality control in the endoplasmic reticulum impairs the biosynthesis of pulmonary surfactant in mice expressing mutant BiP

N Mimura[1,2], H Hamada[3], M Kashio[1], H Jin[1], Y Toyama[4], K Kimura[2], M Iida[5], S Goto[2], H Saisho[2], K Toshimori[4], H Koseki[5] and T Aoe*[,1]

Accumulation of misfolded proteins in the endoplasmic reticulum (ER) induces the unfolded protein response (UPR), which alleviates protein overload in the secretory pathway. Although the UPR is activated under diverse pathological conditions, its physiological role during development and in adulthood has not been fully elucidated. Binding immunoglobulin protein (BiP) is an ER chaperone, which is central to ER function. We produced knock-in mice expressing a mutant BiP lacking the retrieval sequence to cause a defect in ER function without completely eliminating BiP. In embryonic fibroblasts, the UPR compensated for mutation of BiP. However, neonates expressing mutant BiP suffered respiratory failure due to impaired secretion of pulmonary surfactant by alveolar type II epithelial cells. Expression of surfactant protein (SP)-C was reduced and the lamellar body was malformed, indicating that BiP plays a critical role in the biosynthesis of pulmonary surfactant. Because pulmonary surfactant requires extensive post-translational processing in the secretory pathway, these findings suggest that in secretory cells, such as alveolar type II cells, the UPR is essential for managing the normal physiological ER protein overload that occurs during development. Moreover, failure of this adaptive mechanism may increase pulmonary susceptibility to environmental insults, such as hypoxia and ischemia, ultimately leading to neonatal respiratory failure.
Cell Death and Differentiation (2007) 14, 1475–1485; doi:10.1038/sj.cdd.4402151; published online 20 April 2007

Secretory proteins are subjected to quality control in the endoplasmic reticulum (ER) through interaction with molecular chaperones such as binding immunoglobulin protein (BiP), which functions as intermediaries for protein folding or degradation.[1] Extracellular insults, such as ischemia, hypoxia, and genetic mutations, result in aberrant protein folding and accumulation of misfolded proteins in the ER. ER stress initiates the unfolded protein response (UPR), which enhances the capacity for ER quality control by reducing general protein synthesis, producing ER chaperones, and promoting ER-associated protein degradation (ERAD).[2,3] Failure of this adaptive mechanism can cause cellular dysfunction and cell death, resulting in diverse human disorders[4,5] such as neurodegenerative disease, cardiomyopathy,[6] and diabetes.[7]

Respiratory distress syndrome in newborns is often associated with premature birth or low birth weight accompanied by reduced pulmonary surfactant production.[8] Pulmonary surfactant is secreted by highly differentiated alveolar type II epithelial cells, and is composed of phospholipids and surfactant proteins (SP) A, B, C, and D. Surfactant reduces alveolar surface tension and keeps the alveolar space open, which is essential for lung function after the transition at birth from the embryonic fluid environment to air. SP-B and SP-C are small, highly hydrophobic proteins processed from proSP-B and proSP-C, respectively, during transport through the ER and the Golgi to the multivesicular body. Mature SP-B and SP-C are further transported to the lamellar body where they bind phospholipids before secretion into the alveolar space via regulated exocytosis. ProSP-B associated with BiP is found in the ER.[9] Furthermore, mutations in SP-C cause the accumulation of misfolded SP-C in the ER, thereby activating the UPR,[10,11] resulting in interstitial lung disease in children and adults. This suggests that ER stress is involved in lung disease,[12] but whether ER dysfunction causes lung disease remains an open question.

BiP, one of the most abundant ER chaperones, plays a central role in ER function, assisting in protein translocation, folding, degradation, and regulation of the UPR.[13] ER chaperones are localized to the ER by two mechanisms — retention and retrieval.[14] BiP is retained in the ER through interaction with other ER proteins and the ER matrix. When misfolded proteins accumulate in the ER, BiP dissociates from some ER membrane proteins, such as inositol-requiring kinase-1 (IRE1), PKR-like ER-associated kinase (PERK), and activating transcription factor 6 (ATF6). BiP dissociation activates

[1]Department of Anesthesiology, Chiba University Graduate School of Medicine, 1-8-1 Inohana, Chuo-ku, Chiba City, Chiba, Japan; [2]Department of Medicine and Clinical Oncology, Chiba University Graduate School of Medicine, 1-8-1 Inohana, Chuo-ku, Chiba City, Chiba, Japan; [3]Department of Pediatrics, Chiba University Graduate School of Medicine, 1-8-1 Inohana, Chuo-ku, Chiba City, Chiba, Japan; [4]Department of Anatomy and Developmental Biology, Chiba University Graduate School of Medicine, 1-8-1 Inohana, Chuo-ku, Chiba City, Chiba, Japan; [5]Laboratory for Developmental Genetics, RIKEN Research Center for Allergy and Immunology, 1-7-22 Suehiro, Tsurumi, Yokohama, Japan
*Corresponding author: T Aoe, Department of Anesthesiology, Chiba University Graduate School of Medicine, 1-8-1 Inohana, Chuo-ku, Chiba City, Chiba 260-8670, Japan. Tel: +81 43 226 2573; Fax: +81-43-226-2156; E-mail: taoe@faculty.chiba-u.jp
Keywords: chaperone; endoplasmic reticulum; pulmonary surfactant; respiratory failure; UPR
Abbreviations: BiP, binding immunoglobulin protein; ER, endoplasmic reticulum; ERAD, ER-associated protein degradation; MEF, mouse embryonic fibroblast; PAS, periodic acid Schiff; SP, surfactant protein; UPR, unfolded protein response
Received 09.8.06; revised 15.2.07; accepted 16.3.07; Edited by M Piacentini; published online 20.4.07

these kinases and transcription factors and initiates the UPR,[15] which leads to increased expression of X-box-binding protein-1 (XBP-1) and ATF4.[3] When BiP is secreted from the ER along with misfolded proteins,[16,17] the C-terminal Lys-Asp-Glu-Leu (KDEL) sequence of BiP is recognized by the KDEL receptor, thereby facilitating the retrieval of BiP from post-ER compartments to the ER.[18,19] Yeast BiP (Kar2) is essential for survival; when the retrieval sequence (in yeast: His-Asp-Glu-Leu, HDEL) is deleted, a fraction of Kar2 is secreted from the ER. However, the UPR is activated and this maintains a minimal level of Kar2 in the ER.[20]

Complete depletion of BiP could be lethal for early embryonic cells.[21] We therefore produced knock-in mice expressing a mutant BiP in which the retrieval sequence was deleted by homologous recombination. These mice were used to elucidate processes sensitive to ER stress during development and in adulthood. The mutant-BiP mice died several hours after birth. Analysis of neonatal mutants revealed that dedicated secretory systems essential for pulmonary development might include an adaptive mechanism whereby BiP function accommodates increased levels of secretory proteins.

Results

Constitutively active UPR compensates for loss of ER BiP in cultured mammalian cells. We used homologous recombination to produce knock-in mice expressing a mutant BiP lacking the C-terminal KDEL sequence (Figure 1). This mutant BiP contained a C-terminal HA tag. Mouse embryonic fibroblasts (MEFs) derived from homozygous BiP mutant embryos expressed mutant BiP instead of wild-type BiP but grew as well as wild-type MEFs. Mutant BiP localized to the ER, and its expression was enhanced by tunicamycin, which disrupts protein glycosylation in the ER, thereby inducing the UPR. These results are consistent with those for wild-type BiP and other ER chaperones containing a KDEL sequence (Figure 2a). However, in metabolic labeling experiments, a significant fraction of mutant BiP was found in the medium, reflecting deletion of the KDEL sequence and impaired retrieval of mutant BiP (Figure 2b). We estimate that under resting culture conditions, one-third of the newly synthesized mutant BiP was secreted. The remainder was retained in the ER. A fraction of wild-type BiP was also secreted into the medium during ER stress (tunicamycin treatment), indicating that retrieval by the KDEL receptor is saturable.

Tunicamycin sensitivity and expression of mutant BiP was also confirmed by Western blotting (Figure 3a and b). Both mutant BiP and wild-type BiP were recognized by an antibody against the N-terminus of BiP. However, anti-KDEL only recognized wild-type BiP and GRP94, an ER chaperone with the KDEL sequence. Basal expression of XBP1, ATF4, phospho-PERK, and another ER chaperone, calreticulin, was enhanced in homozygous mutant BiP MEFs. Basal expression of mutant BiP mRNA was also enhanced in mutant MEFs (Figure 3c), indicating that the UPR was constitutively active. Thus, as seen previously in yeast,[20] constitutive UPR activation maintains a minimal level of BiP (mutant or wild type) in the ER of mammalian cells, thus compensating for deletion of the KDEL sequence.

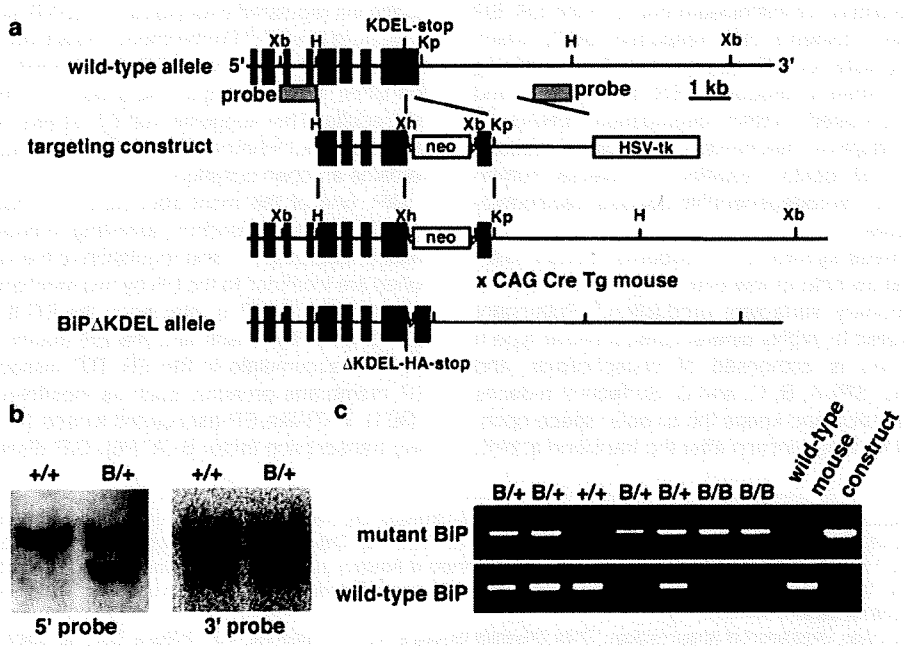

Figure 1 Generation of knock-in mice expressing a mutant BiP lacking the KDEL retrieval sequence. (**a**) Top, the wild-type allele containing the BiP gene. Exons are indicated as solid bars. Middle, the targeting vector for homologous recombination. Bottom, the recombinant allele. The external probes for Southern blot analysis are indicated by gray quadrangle. Xb, *Xba*I; H, *Hind*III; B, *Bam*HI; Kp, *Kpn*I; Xh, *Xho*I. (**b**) Southern blots of ES cell genomic DNA digested with *Xba*I. The 5′ external probe detected a 11.2-kb fragment in the wild-type allele and a 4.7-kb fragment in the mutant allele. The 3′ external probe detected a 11.2-kb fragment in the wild-type allele and a 8.0-kb fragment in the mutant allele. '+' represents the wild-type allele, and 'B' represents the mutant allele. (**c**) Genotyping of mice by PCR

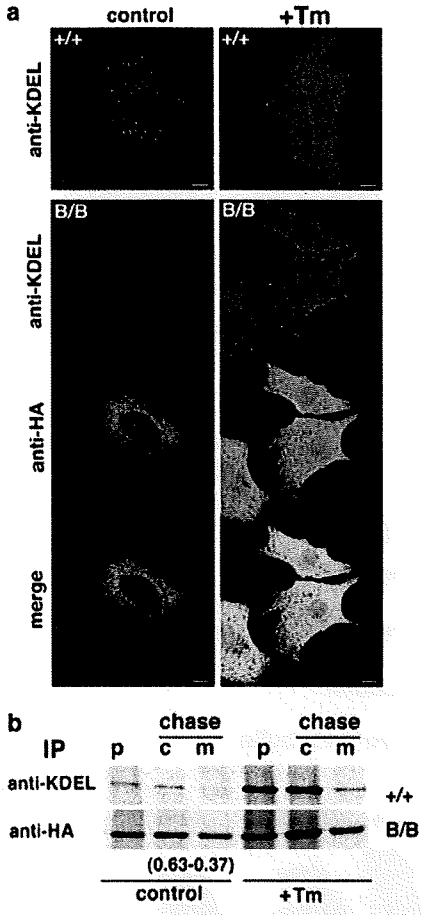

Figure 2 Deletion of the KDEL sequence impairs retrieval of mutant BiP. (**a**) MEFs from homozygous mutant (B/B) and wild-type (+/+) embryos treated with or without tunicamycin (Tm, 2.5 μg ml^{-1}) for 12 h were double-stained with monoclonal anti-KDEL and polyclonal anti-HA and observed by confocal laser microscopy. The anti-KDEL recognizes BiP as well as other KDEL-containing proteins, such as GRP94. Scale bars represent 10 μm. (**b**) Tm-treated (2.5 μg ml^{-1} for 12 h) or untreated MEFs were subjected to pulse-chase (p and c) labeling with[35S]methionine. Proteins in cell lysates (p and c) and in the culture medium (m) were immunoprecipitated with anti-KDEL or anti-HA. The proportion of secreted mutant BiP (m; 0.37) was evaluated by densitometry

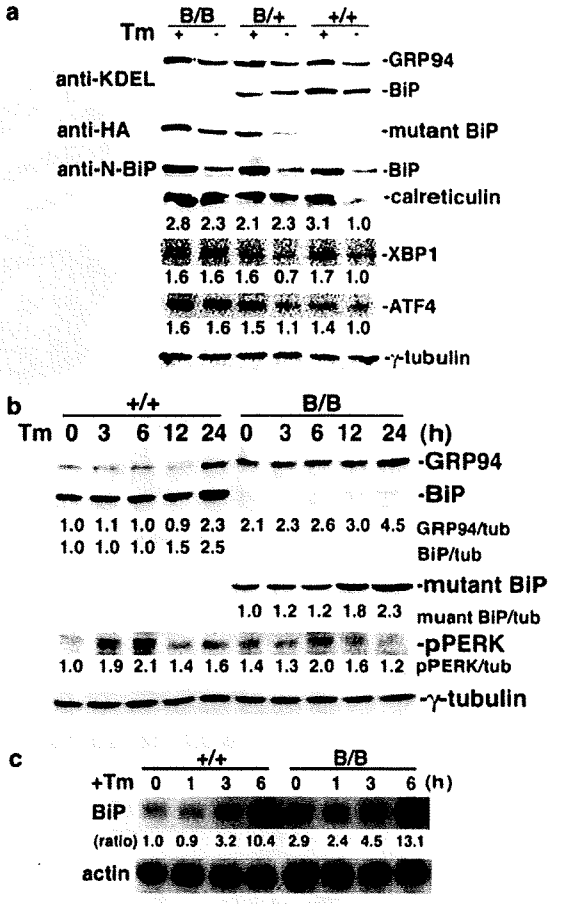

Figure 3 Loss of wild-type BiP is compensated by constitutive activation of the UPR in mammalian cells. (**a**) Tunicamycin (Tm)-treated (2.5 μg ml^{-1} for 12 h) or untreated MEFs from homozygous (B/B), heterozygous (B/+) and wild-type (+/+) embryos were collected. Expression of BiP, GRP94, mutant BiP, calreticulin, XBP1, ATF4, and γ-tubulin was determined by Western blotting. (**b**) Tm-treated (2.5 μg ml^{-1} for 0, 3, 6, 12, and 24 h) MEFs from homozygous (B/B) and wild-type (+/+) embryos were collected. Expression of BiP, GRP94, mutant BiP, phospho-PERK, and γ-tubulin was determined by Western blotting. The expression of each protein was normalized to that of γ-tubulin. (**c**) Northern blot of BiP mRNA expression in MEFs from homozygous (B/B) and wild-type (+/+) embryos treated with Tm (2.5 μg ml^{-1}) at 37°C for 0–6 h. The expression of BiP mRNA was normalized to that of β-actin mRNA

Mutant-BiP embryos die shortly after birth. BiP was ubiquitously expressed in both mutant and wild-type embryos (Figure 4a and b). In all tissues examined, GRP94 expression was greater in homozygous BiP mutant embryos than in wild-type embryos (Figure 4b), suggesting that homozygous BiP mutant mice may suffer from global ER stress. Homozygous mutant-BiP embryos weighed less than wild types and heterozygotes at embryonic day (E) 18.5 (Figure 4c). Homozygous BiP mutant mice, shown in Figure 4d, were born at the expected Mendelian ratio of 1:2:1 (84:182:90, wild type:heterozygous:homozygous). Neonatal BiP mutants moved well and responded to painful stimuli, but they appeared pale and cyanotic. They also cried less and displayed shallow breathing. The neonatal homozygous mutants generally died within several hours of birth; thus, we suspected that the observed lethality might reflect respiratory problems.

When delivered by Caesarian section at E18.5 and killed before breathing, gross morphology of the lungs (Figure 4e) and airways from BiP mutant mice was indistinguishable from wild type (Figure 5a). Wild-type and homozygous BiP mutant embryonic alveoli had an equivalent distribution of alveolar type II cells expressing the SP-C (Figure 5b). However, histological examination of lungs isolated from neonatal BiP mutants several hours after birth revealed atelectasis with poor inflation of peripheral airways. Hemorrhage and cell debris were also observed in the mutant alveolar space. Alveolar epithelia in BiP mutant mice were enlarged, whereas, as expected, those in wild-type neonates were distended

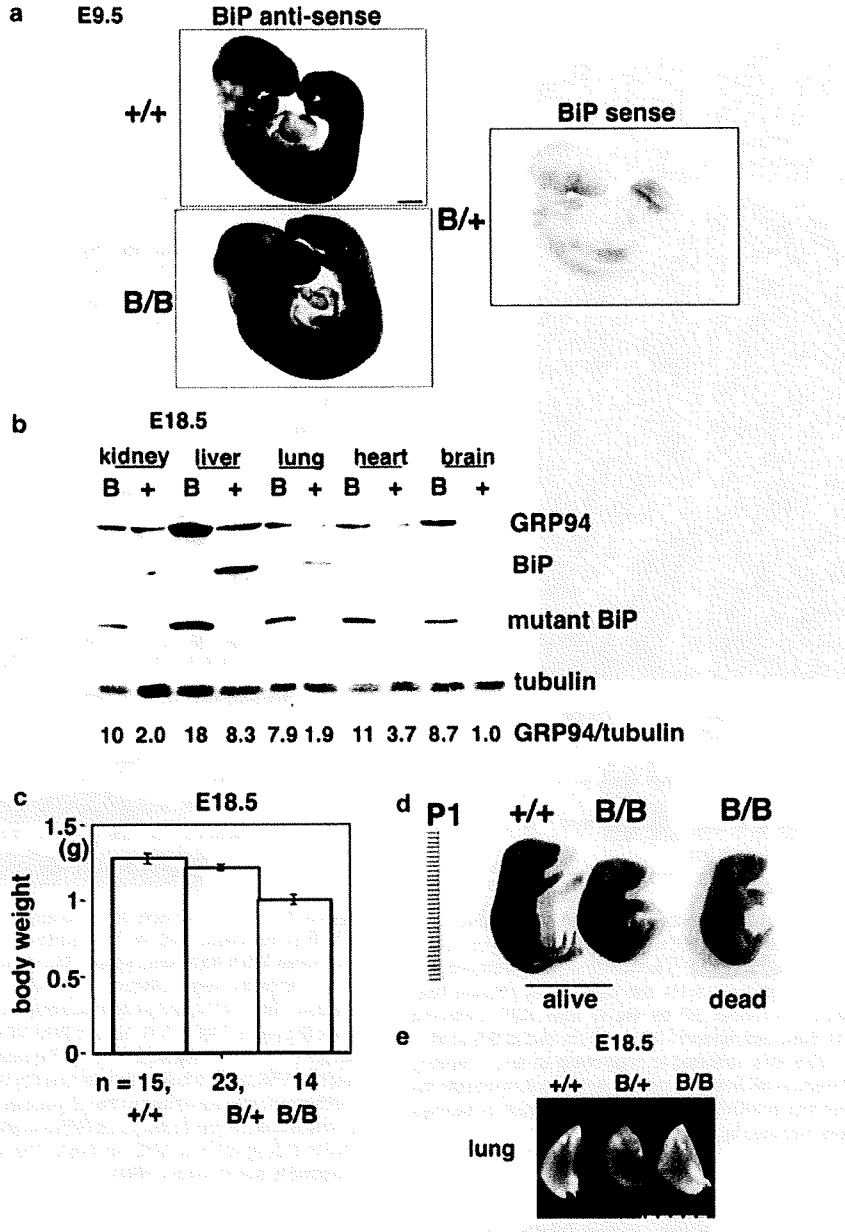

Figure 4 Mutant-BiP embryos die shortly after birth. (**a**) BiP expression was ubiquitous in both mutant and wild-type embryos. Whole-mount *in situ* hybridization revealed ubiquitous expression of BiP and mutant BiP in E9.5 embryos. Scale bar represents 200 μm. (**b**) Western blots of BiP or mutant-BiP in tissues from wild type (+) and homozygous mutant (**b**) E18.5 embryos, respectively. Expression of GRP94 was normalized to that of γ-tubulin. In all tissues examined, GRP94 was greater in mutants than in wild type. (**c**) Body weights (mean $\pm$ S.D.) of homozygous (B/B, $n=14$), heterozygous (B/+, $n=23$) and wild-type (+/+, $n=15$) E18.5 embryos. Homozygous mutant embryos weighed significantly less than wild types or heterozygotes ($P<0.0001$). (**d**) Gross appearance of wild type (+/+) and homozygous (B/B) P1 neonates. (**e**) Lungs from E18.5 mice delivered by Cesarian section

(Figure 5c). These observations indicate that homozygous neonatal BiP mutants developed atelectasis and respiratory failure after birth.

Altered biosynthesis of SPs in mutant alveolar type II cells. To examine whether a deficiency of pulmonary surfactant contributes to respiratory failure in homozygous BiP mutant mice, perfluorocarbon, a substitute for pulmonary surfactant, was administered into the oropharynx. Perfluorocarbon with oxygen treatment improved the activity of neonatal BiP mutants, turned their skin color from pale to pink, and improved lung inflation (Figure 5d). Expression of SPs in neonatal lung was examined by Western blotting (Figure 6a). Expression of SP-A and, more prominently,

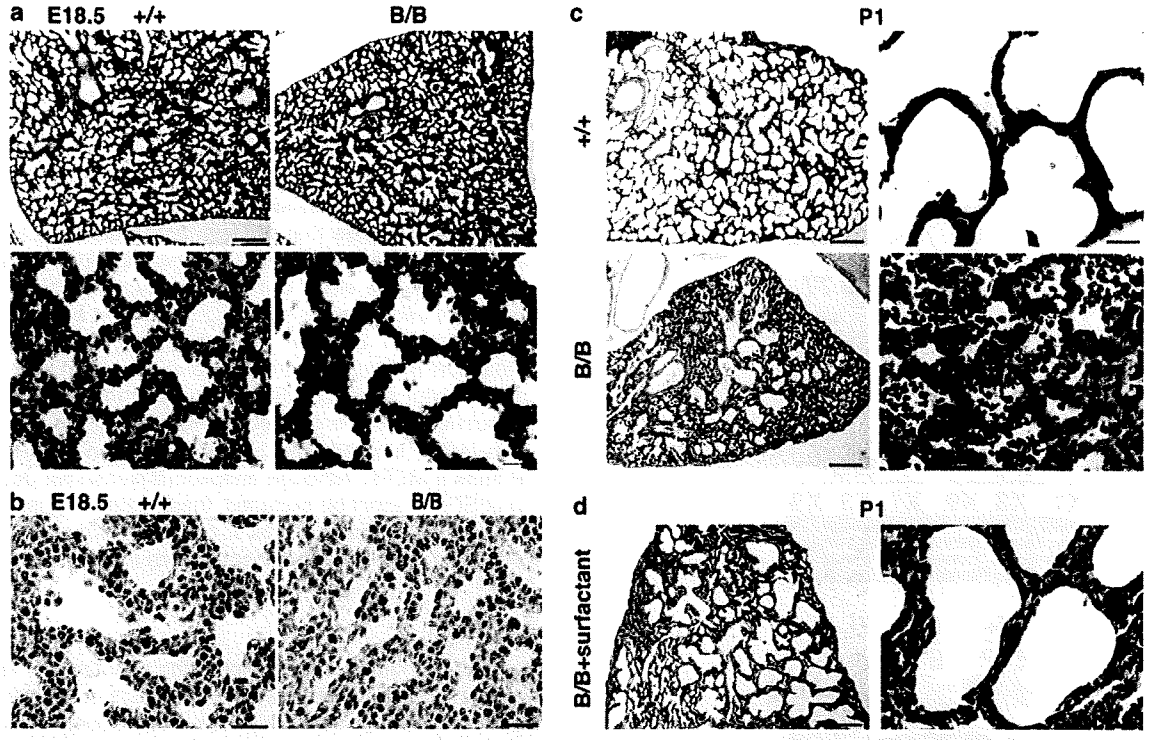

Figure 5 The gross morphology of lungs and airways from BiP mutant embryos is indistinguishable from wild type. (**a, b**) Lungs from E18.5 mice delivered by Cesarian section. (**a**) Sections stained with hematoxylin and eosin. +/+: wild-type, B/B: homozygous mutant. (**b**) Alveolar type II epithelial cells were stained with anti-SP-C (brown). Nuclei were stained with hematoxylin (violet). (**c**) Lung sections from P1 neonates. Atelectasis and cell debris were evident in the peripheral airways of neonatal mutants. +/+: Wild-type, B/B: homozygous mutant. (**d**) Lungs from a P1 neonatal BiP mutant (B/B) administered 50 μl of perfluorocarbon via the oropharynx and treated with 40% oxygen for 6 h. Sections were stained with hematoxylin and eosin. Scale bars represent 200 and 20 μm in the low- and high-magnification images, respectively

proSP-C, was reduced in mutant lungs compared with wild type, but there was no significant difference in proSP-B and SP-D expression. RT-PCR analysis revealed that the marked reduction of proSP-C in neonatal mutant lung was not due to reduced transcription (Figure 6b). Importantly, after birth, the expression of proSP-C was enhanced only in wild-type neonates (Figure 6c), suggesting that proSP-C might be degraded post-translationally in neonatal type II cells from BiP mutants. Furthermore, expression of CHOP, a transcription factor related to cell death during ER stress,[22] increased in homozygous mutant lungs after birth, suggesting that mutant lung tissue might be suffering from ER stress. Heterozygous BiP mutants were viable and grew to adulthood. Furthermore, heterozygous expression of wild-type BiP sustained SP-C expression and suppressed CHOP expression in lung (Figure 6d and e), suggesting that the wild-type BiP is essential for SP-C biosynthesis.

The subcellular localization of SP-A and SP-C was evaluated by confocal laser microscopy. In wild-type neonatal alveolar type II cells, SP-A and SP-C (proSP-C) colocalized with BiP, and other KDEL sequence–containing ER chaperones, in the ER. SP-A accumulated in the alveolar lining area of BiP mutant mice and costained with mutant BiP (Figure 7a). By contrast, SP-C remained in the ER, and its expression was markedly reduced in type II cells of neonatal BiP mutants (Figure 7b). Mature SP-B and SP-C are transported to the lamellar body where they bind phospholipids and are then secreted into the alveolar space via regulated exocytosis, whereas SP-A and SP-D are secreted independently of the lamellar body.[12] Together, these data suggest that mutant BiP impairs the secretion of pulmonary surfactant, especially secretion through the lamellar body.

Embryonic type II cells store glycogen in the cytoplasm, and this glycogen is consumed as the synthesis of pulmonary surfactant expands after birth. Type II cells in neonatal BiP mutants contained vacuole structures. Periodic acid Schiff (PAS) staining revealed cytoplasmic polysaccharides in these cells, even after birth (Figure 8a). Ultrastructural analysis of type II cells from neonates confirmed that cytoplasmic glycogen was indeed still present in mutant, but not in wild type, cells (Figure 8b and c). More importantly, the structure of the lamellar body was abnormal in embryonic and neonatal mutant type II cells. The lamellar body in wild-type neonates had wavy, dense laminations with clefting, whereas in BiP mutant neonates the lamellar body had loosely formed lamellar structures or was almost empty. These results indicate that the biosynthesis and secretion of pulmonary surfactant was impaired in BiP mutant type II cells.

SP-C is a small, highly hydrophobic protein processed from proSP-C during its transport through the ER and the Golgi to the multivesicular body. Mature SP-C is transported further to the lamellar body where it binds phospholipids before

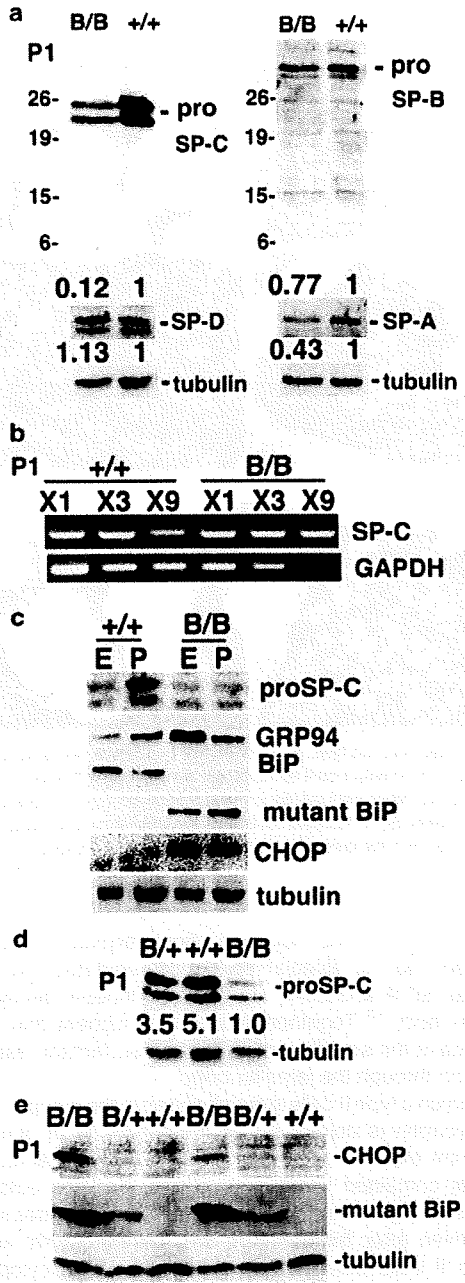

Figure 6 Biosynthesis of pulmonary surfactant is impaired in mutant-BiP lung. (**a**) Western blots of SP-A, SP-B (proSP-B), SP-C (proSP-C), SP-D and γ-tubulin in lungs from P1 wild types (+/+) and mutants (B/B). The expression of each protein was normalized to that of γ-tubulin. (**b**) SP-C mRNA in lungs from P1 wild-types (+/+) and mutants (B/B) was evaluated by semi-quantitative RT-PCR. Serial dilutions of cDNA were standardized to GAPDH. (**c**) Western blots of pro-SP-C, GRP94, BiP, mutant BiP, CHOP, and γ-tubulin in lungs from E18.5 (E) and P1 (P) mice. (**d**) Western blots of SP-C (proSP-C) and γ-tubulin in lungs from P1 wild-type (+/+), heterozygous (B/+), and homozygous (B/B) mutant mice. The expression of SP-C was normalized to that of γ-tubulin. (**e**) Western blots of mutant BiP, CHOP, and γ-tubulin in P1 lungs

secretion into alveolar space via regulated exocytosis. Lamellar body formation is defective in alveolar type II cells of neonatal BiP mutants. Therefore, SP-C may be degraded by endosomal/lysosomal degradation and/or the ERAD pathway. Punctate SP-C is colocalized with KDEL-containing ER chaperones in both wild-type and homozygous mutant type II cells (Figure 9a), suggestive of ER accumulation of SP-C. The fraction of ER accumulation of SP-C in the mutant type II cells was 0.84, while that of Golgi accumulation was 0.08, evaluated by confocal colocalization images (Figure 9a and b).

To examine the effect of proteasome inhibitors on SP-C, MEFs from wild-type and homozygous mutant embryos were transfected with SP-C in the presence or absence of a proteasome inhibitor (Figure 9c and d). Although the proteasome inhibitor enhanced SP-C expression in wild-type and BiP mutant MEFs, it enhanced surface expression of SP-C in wild-type MEFs but promoted ER accumulation of SP-C in the BiP mutant MEFs. Although endosomal/lysosomal degradation of SP-C cannot be excluded, these data suggest that, in homozygous mutant-BiP type II cells, misfolded SP-C may accumulate in the ER and be degraded by the ERAD pathway.

Discussion

We produced knock-in mice expressing a mutant BiP lacking the retrieval sequence to examine the effects of defects in the secretory pathway stress response without completely eliminating BiP function—as would be the case in BiP knockout mice.[21] Mutant BiP predominantly affected dedicated secretory cells, such as alveolar type II cells, in which active secretion is particularly important. Putative impairment of protein folding in these mutant cells probably caused the observed respiratory failure and high neonatal mortality.

Deletion of the retrieval sequence from BiP, and the consequent lack of mutant-BiP recycling, could have two possible effects. First, the folding environment in the ER may be impaired. However, mutant BiP is functional as long as it remains in the ER. Therefore, constitutive activation of the UPR could compensate for the altered folding environment by producing mutant BiP in quantities sufficient for cell survival. Second, quality control in post-ER compartments may be affected. Proper ER-to-Golgi transport and subsequent ER retrieval of proteins and lipids is thought to contribute to quality control.[16,17,23] In this regard, the folding (and therefore function) of pulmonary SPs, especially proSP-C, may depend on proper ER retrieval of BiP via the KDEL receptor.

Respiratory distress syndrome of newborns, also called hyaline membrane disease, causes high mortality and often accompanies pre-term delivery or low birth weight with reduced expression of pulmonary surfactant. Surfactant therapy combined with mechanical ventilation and other intensive care measures has reduced the mortality rate of this syndrome to below 10%.[24] Surfactant proteins are required for proper lung development and function. Respiratory diseases result in humans and other mammals when these proteins are lacking. SP-B is critical for lung surfactant formation and function, and its deficiency causes immediate and severe neonatal respiratory failure in humans and mice.[25,26] Deletion of SP-B induces aberrant processing of proSP-C as well as defects in lamellar body formation. SP-C

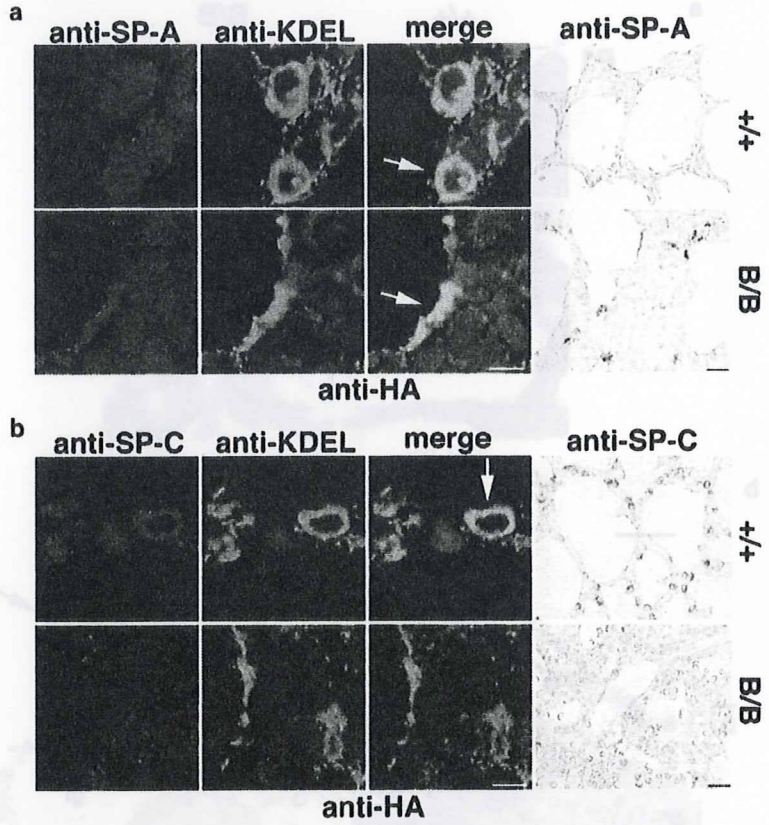

Figure 7 SP-A and SP-C in lungs from BiP mutants. (**a**) Costaining of lungs from P1 wild-type (+/+) and mutant (B/B) mice with anti-SP-A (brown staining, right panels) and monoclonal anti-KDEL or anti-HA (shown in green in different panels). (**b**) Costaining of lungs from P1 wild types (+/+) and mutants (B/B) with anti-SP-C (proSP-C; right panels) and anti-KDEL or anti-HA. Arrows indicate colocalization of SP-A or SP-C with KDEL-containing chaperones in wild-type type II cells as well as colocalization of SP-A with mutant BiP in B/B type II cells

deficits are related to acute and chronic infant lung diseases in humans[27] and respiratory failure in cattle.[28] Furthermore, mutations in proSP-C have been correlated with chronic interstitial pneumonia.[11,12] ProSP-C is an type II integral membrane protein with structural homology to the amyloidogenic BRI family of proteins, which cause neurodegenerative dementia.[29] Mutant proSP-C tends to misfold and may cause protein aggregation and ER stress.[12] Thus, in the present study, aberrant quality control in the mutant-BiP type II epithelial cells may have resulted in proSP-C misfolding. Misfolded proSP-C may act in concert with decreased pulmonary surfactant levels to generate respiratory failure by causing ER stress in mutant type II cells.

Mutant-BiP mice have a distinct phenotype, as is the case for mice lacking other ER molecular chaperones. Hsp47 is responsible for collagen biosynthesis, and Hsp47 knockout mice die on E11.5.[30] Calreticulin and calnexin participate in glycoprotein folding in the ER. Calreticulin knockout mice are embryonic lethal and display defective cardiac development.[31] Calnexin knockout mice die during the early postnatal period, between birth and 3 months of age. These mice exhibit motor disorders owing to a loss of large myelinated nerve fibers.[32]

The UPR is a ubiquitous mechanism for adapting to ER stress, and BiP is an essential component of this system. However, at various developmental stages, some cell types require specific UPR signaling systems[33] and chaperones. Mutant mouse models have revealed that the UPR plays a vital role during development by increasing protein synthesis as needed in dedicated secretory cells,[34] such as pancreatic β cells,[35] plasma cells[36] and hepatocytes.[37] Inadequate adaptation to these types of physiological demands may lead to diverse diseases.

Diminished quality control in the ER and in post-ER compartments of the mutant-BiP alveolar type II cells may be sufficient embryonically but not neonatally when increased biosynthesis of proSP-C and other SPs requires sufficient folding capacity. Indeed, at E18.5, proSP-C expression in type II cells was equivalent in lungs from BiP mutants and wild types (Figures 5b and 6c). After birth, proSP-C expression increased markedly in wild-type lungs but not in mutant lungs. SP-C mRNA level was, however, preserved in the BiP mutants, suggesting that proSP-C may be degraded co- or post-translationally in neonatal mutants.

Our results suggest that in neonates a physiological increase in SP production causes ER stress in dedicated secretory cells, like alveolar type II epithelial cells. This may increase susceptibility to environmental insults such as hypoxia and ischemia, leading to respiratory failure due to the

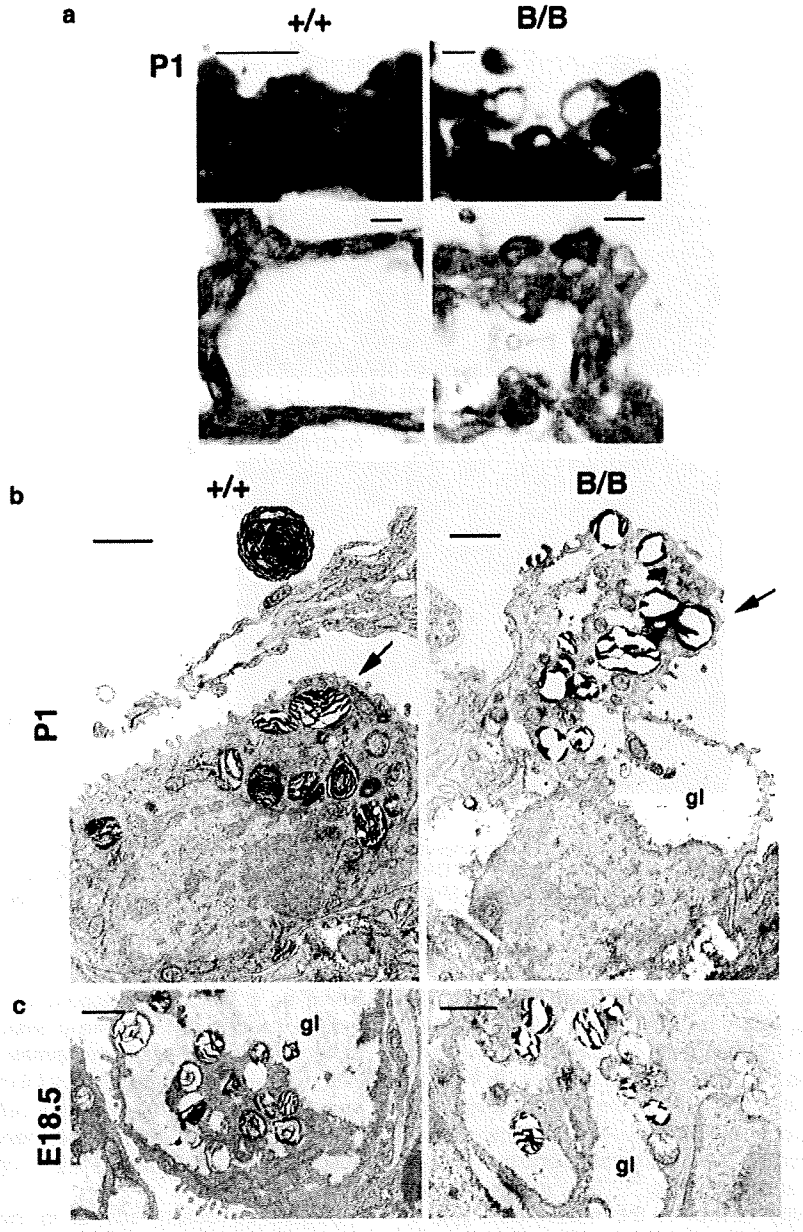

Figure 8 Defective lamellar body formation in neonatal mutant-BiP alveolar type II cells. (**a**) Neonatal mutant type II cells contained vacuole structures. Alveolar epithelium from P1 wild type (+/+) and mutant (B/B) mice stained with toluidine blue (upper panels) or PAS (lower panels). Scale bars represent 10 μm. (**b**, **c**) Ultrastructure of the alveolar epithelium from wild type (+/+) and mutant-BiP (B/B) P1 neonates (**b**) and E18.5 embryos (**c**). Scale bars represent 1 μm. Arrows indicate lamellar bodies in type II cells. Cytoplasmic glycogen (gl) remained in neonatal mutant type II cells

loss of pulmonary surfactant and accumulation of misfolded proteins in the ER.

Materials and Methods

Cells, reagents, and general procedures. MEFs were prepared from E13.5 embryos. MEFs were grown at 37°C in an atmosphere of 5% CO_2 in complete medium consisting of Dulbecco's modified essential medium (DMEM; Sigma Chemical Co.) with 15% fetal bovine serum (FBS), 2 mM glutamine, 50 μg ml^{-1} streptomycin and 50 U ml^{-1} penicillin G.

The following antibodies were used: rabbit antiserum against calreticulin (Affinity Bioreagent), rabbit antiserum against XBP-1, rabbit antiserum against ATF4, rabbit antiserum against CHOP/GADD153, goat polyclonal antiserum against BiP/GRP78, rabbit antiserum against SP-A (H-148), goat polyclonal antiserum against SP-B (R-19), rabbit antiserum against SP-C (FL-197), rabbit antiserum against SP-D (C-18), rabbit antiserum against ubiquitin (all from Santa Cruz Biotechnology), rabbit anti-serum against the HA epitope (Zymed), mouse monoclonal antibody (mAb) against γ-tubulin (Sigma Chemical), mouse mAb SPA-827 against BiP (KDEL sequence; Stressgen), mouse mAb G1/133 against giantin (Alexis Biochemicals), Cy-2- or Cy-3-conjugated donkey antibody against rabbit IgG, and Cy-2- or

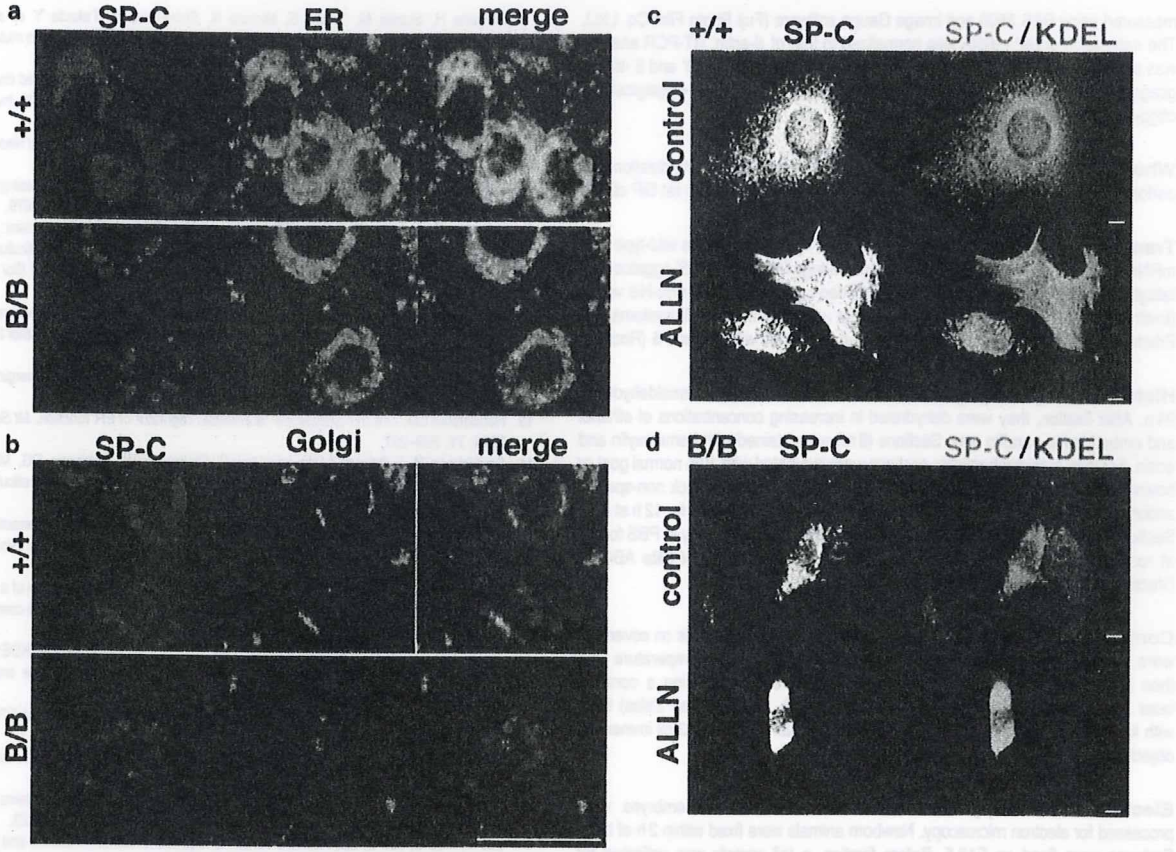

Figure 9 SP-C accumulation in the ER. (**a**) Lungs from a P1 wild-type neonate (+/+) and a homozygous mutant (B/B) costained with polyclonal anti-SP-C and monoclonal anti-KDEL (ER staining). Colocalization of SP-C with KDEL-containing ER chaperones was seen in both wild type and mutant alveolar type II cells. (**b**) Lungs from a P1 wild-type neonate (+/+) and a homozygous mutant (B/B) co-stained with polyclonal anti-SP-C and monoclonal anti-giantin (Golgi complex staining). Scale bar represents 10 μm. The fractions of ER-localizing SP-C and Golgi-localizing SP-C were calculated by confocal colocalization images. ER-localizing SP-C to total SP-C in wild type; 0.81 ± 0.052, Golgi-localizing SP-C in wild type; 0.12 ± 0.032, ER-localizing SP-C in mutant; 0.84 ± 0.036 (significantly more than that of wild types by *t*-test, $P < 0.018$), Golgi-localizing SP-C in mutant; 0.08 ± 0.043 (significantly less than that of wild types, $P < 0.0015$). $n = 20$, mean $\pm$ S.D. (**c, d**) Inhibition of proteasomal degradation promotes ER accumulation of SP-C in homozygous mutant MEFs. MEFs from wild type (+/+, **c**) and homozygous mutant (B/B, **d**) embryos were transfected with SP-C with or without ALLN (10 μg ml^{-1}; 12 h) then double-stained with monoclonal anti-KDEL (red) and polyclonal anti-SP-C (green). Anti-KDEL recognizes BiP as well as other KDEL-containing proteins, such as GRP94. Scale bars represent 10 μm

Cy-3-conjugated donkey antibody against mouse IgG (Jackson Immunoresearch Laboratories). Tunicamycin was purchased from Nacali Tasque. Perfluorocarbon (perfluoro-2-butyltetrahydrofuran) was purchased from Fluorochem. *N*-acetyl-l-leucinal-l-lecinal-l-norleucinal (ALLN) was purchased from Sigma Chemical.

Metabolic labeling experiments and Western blotting were performed as described previously.[6] Densitometry was performed using BAS 2500 and Image Gauge software (Fuji Photo Film Co., Ltd.) for metabolic labeling experiments and using LAS 1000 (Fuji Photo Film Co., Ltd.) and ImageJ software (Wayne Rasband, NIH) for Western blotting.

Generating mutant-BiP mice. All animal experimental procedures were in accordance with a protocol approved by the Institutional Animal Care Committee of Chiba University, Chiba, Japan. A rat BiP cDNA was used as a probe to isolate a genomic clone containing the whole exon of the BiP gene[38] from the 129/SvJ mouse genomic library in λFIXII (Stratagene). A 0.6-kb *Bam*HI/*Xho*I fragment encoding the C-terminal end of BiP and the stop codon, but lacking the KDEL sequence, was obtained by PCR. Then, part of a 2.1-kb genomic fragment containing the last three exons was replaced by the 0.6-kb fragment. The resultant fragment was used as a short arm for the targeting vector. A 0.5-kb *Xba*I/*Kpn*I fragment, encoding the 3′ untranslated region of the exon after the stop codon and the 2.5-kb intron that followed, was amplified by a PCR and used as a long arm for the targeting vector. An *Xho*I/*Xba*I fragment containing a neomycin selection cassette flanked by *lox*P sequences (PHR68, a gift from T Kondo, Saitama, Japan) and a 2.7-kb fragment containing the HSV-thymidine kinase gene were introduced into the targeting vector to allow negative and positive selection. The targeting vector was linearized with *Not*I digestion and used for electroporation into R1 ES cells. The mutant allele resulting from homologous recombination had artificial *Xho*I and *Xba*I sites. Genomic DNA from G418-resistant clones (G418 was from Life Technologies) was digested with *Xba*I and analyzed by Southern blotting using an *Xba*I/*Hin*dIII fragment for the 5′-end probe and a PCR-amplified fragment for the 3′-end probe, as shown in Figure 1. Several homologous recombinants were obtained, and germline chimeras were generated as described.[39] Resulting male chimeras were mated to C57BL/6 females. Tail DNA from the offspring was screened by PCR using the following oligonucleotides: 5′-gatcagtgcacctacaactc-3′ and 5′-gctcaaagagcgcattgac-3′ for the wild-type allele, and 5′-gtgaacgacccctaacaa aa-3′ and 5′-agcgtaatctggaacatcgt-3′ for the recombinant allele. To remove the neomycin selection cassette, heterozygous mice were mated with mice expressing Cre under the control of a CAG promoter. Heterozygous mice lacking neomycin were interbred to obtain homozygous mutant mice.

Detection of mRNA. Northern blot analysis was carried out as described.[6] Expression of BiP and β-actin mRNAs was evaluated using cDNA probes encoding rat BiP (a gift from Dr. HRB Pelham) and mouse β-actin. Radioactivity was